
FLUID INCLUSIONS TECHNIQUE FOR PORPHYRY DEPOSIT EXPLORATION: THE ROSARIO PORPHYRY CU-MO DEPOSIT

A PREPRINT

Nicolas Avalos
Department of Geology
University of Chile
Plaza Ercilla 803, Santiago, Chile
nicolas.avalos@ing.uchile.cl

Sebastian Avalos
Advanced Predictive Modeling Technology
Kingston, Canada
sebastian.avalos@apmodtech.com

May 15, 2023

This is a non-peer reviewed preprint submitted to EarthArXiv

ABSTRACT

Porphyry ore deposits are the largest source of copper, molybdenum, gold, and silver in the world. Various exploration techniques have been developed due to their importance as a source of metals. A special focus has been devoted to understanding the processes of hydrothermal fluids as mineralization drivers. Fluid inclusions provide direct information about the fluids involved in the hydrothermal genesis of the ore deposit. They convey temperature and mineral composition information conditioned to the salinity of the fluid system. Thus, fluid inclusion analysis works as an additional tool for porphyry ore deposit exploration.

We present a new exploration technique based on the properties of PVTX fluids to find porphyry copper. The Collahuasi district located in the North of Chile has 2 currently exploited and known porphyry: Rosario and Ujina porphyries. The investigation was carried out around the Rosario porphyry, which has reserves estimated at 2.18 BTon (0.91% Cu). Potassium, propylitic, quartz-sericite, argillic and advanced argillic alteration have been identified in this area. The latter was associated with high sulfidation veins, possibly related to a second unknown intrusion, named the Rosario Oeste zone.

The petrographic study of fluid inclusions was carried out on more than 300 drilling samples from Rosario and Rosario Oeste. 7 classifications of the types of FI that occur, these are: liquid-rich fluid inclusions, FI steam-rich, FI with coexistence of liquid and vapour, FI rich in liquid with halite, FI liquid-rich with halite coexisting with vapour, FI rich in liquid with chalcopyrite and FI with solids. The veins were classified with the support of the Collahuasi geology team, as veins type A, B, C, D, E, TES, and only quartz. The main alterations defined to use were: propylitic and argillic.

This information, an exploration model called the Copper Porphyry Probability Index (CPPI) is generated. All this information was integrated into a 2D and 3D model to study the spatial distribution of these parameters. It is concluded that boiling is present throughout the system in the upper and lower zones. Higher salinity and metal content in the fluid are recognized, positively correlating with the presence of type B and D veins and with high CPPI values, showing these in the direction of Rosario Oeste.

These similarities in shallow and deep parts, which correlate with two high-grade Cu-Mo zones, suggest the presence of two simultaneous mineralizing centers or the possibility of recurrent mineralization by a low-angle structural process.

Keywords Fluid inclusions · Porphyry ore deposits · Mineralization · Exploration

1 Introduction

Porphyry ore deposits are the largest source of copper in the world (Singer et al., 2002; Sillitoe, 2010). Several exploration techniques have been developed to increase the probability of finding new deposits based mainly on a deep understanding of the ore metallogenesis. In that sense, geological system knowledge associated with their metallogenesis points as key-driven sources: tectonic environments, mineral alterations, structural veins and zones of mineralization, and even the metal kinetics of transportation and concentration (Burnham, 1979; Hedenquist and Lowenstern, 1994; Beane and Bodnar, 1995; Singer et al., 2002; Sillitoe, 2010; Zajacz et al., 2017).

The study of Fluid Inclusions (FI) appears as an additional source of information which involves the analysis of metals embedded or trapped in the fluids during the rock genesis. Commonly, the scope of FI reports in porphyry copper deposits has been to validate the environmental conditions of their genesis, through microthermometry, due to the presence of magmatic-hydrothermal fluids during their evolution (Burnham, 1979; Roedder, 1972). Seeking to establish the study of FI as an additional tool for exploration. Nash (1976) and Bodnar (1982) have compiled literature reviews of FI to make them useful as an independent and manageable source of information about ore body genesis

This work complements the previous efforts by gathering the theoretical principles of fluid inclusions found in Roedder (1984); Van den Kerkhof and Hein (2001); Goldstein and Samson (2003); Bodnar et al. (1985), compiling the current theoretical backgrounds of FI and their relationships with porphyry copper deposits. In addition, a practical petrographic case of study is carried out in a real porphyry copper deposit in Chile. Here, seven type of FI were defined and studied by petrographic analysis at room temperature. Additionally, a synthetic index is built at each sample based on the abundance of the three main kind of FI. The information is then spatially located into geological sections to enrich the database by including a realistic and practical visual analysis. By doing so, the use of FI are supported by merging (1) theoretical approaches, (2) practical aspects, and (3) validation over a real porphyry copper deposit. As a result, inferences of transport mechanisms and precipitations, fluid conditions, spatial distributions, and other representative characteristics are obtained.

2 Methodology

Fluid inclusions studies can be broken down into four key stages: (i) theoretical background, (ii) data collection, (iii) comparative analysis, and (iv) feasibility analysis. Figure 1 illustrates the stage connectivity.

A brief description of each stage and the particular settings to our case of study are found below.

Theoretical background Gathering information on petrographic observations of fluid inclusions in porphyry copper deposit explorations. Guidelines derived from these background are specified to a particular deposit. The following data collection process is driven by those theoretical guidelines in terms of drill-hole campaign.

Data collection Gathering representative samples of the ore deposit. Observations of fluid inclusions are derived from quick-plates cutting over the collected samples. This observations account for the diversity in types of fluid inclusions. Based on the relative abundance of (i) inclusions rich in vapour, (ii) inclusions with presence of halite, and (iii) inclusions containing chalcopyrite, a cupriferous porphyry probability index (CPPI) Bodnar (1982); Roedder (1997) value is assigned to each sample.

Comparative analysis The theory is contrasted with the real obtained information. Once the CPPI and fluid types are associated to each sample, a comparative analysis is carried out using the samples coordinates, geological sections of the ore deposit and other known deposits with similar genesis.

Feasibility analysis Establishing the feasibility of using FI as a key driver in porphyry copper deposit explorations. Once the collected samples have been contrasted with the theory, similar deposits and external geological information of the same deposit, the feasibility of using FI in the deposit exploration is made.

3 Geology setting

Collahuasi district is located the First Region of northern Chile, five to ten km with the respect to the country limit with Bolivia. Located within a horst of Mesozoic and Paleozoic rocks, raised in the Upper Tertiary, it corresponds to a block that has 30 km of north-south elongation and 40km of west-east width, limited to the west by the Domeyko Range along with the Domeyko Fault System and to the east by the Western Cordillera. In its center, the structural dynamics are driven by two major faults that show an NNW-SSE orientation, and several minor faults with NE-SW, NW-SE and N-S orientations Munchmeyer et al. (1984). The major NNW-SSE faults, with regional extension, are *West Fault* and *Loa Fault*.

Three main stratigraphic domains, driven by structural control, are defined by the Domeyko fault system as the west limit and the Loa fault system as the eastern limit. The Collahuasi Formation is located in the middle of both fault systems in which the Rosario Porphyry is situated. It is worth mentioning that the Domeyko fault system circumscribes a large portion of copper deposits in north of Chile, including Chuquibambilla, Escondida and Salvador [Camus \(2002\)](#).

The Cerro Empexa formation and the Quehuita Formation are situated at the west of the Domeyko fault system, and ignimbrites are distributed to the east of the Loa Fault and in a north-south direction with respect to the Loa Fault [Bisso et al. \(1998\)](#). Within these stratified domains, stratum volcanoes, unconsolidated deposits, terraced deposits and a series of various intrusives can be found

3.1 Stratified lithologies

Four major stratified lithologies are found in the district: Collahuasi formation, Quehuita formation, Cerro Empexa formation and Cenozoic rocks.

Collahuasi formation Permo-Triassic age formation (229-221 Ma) composed of andesites, dacites, rhyolites, tuffs and porphyry intrusive bodies. The volcanic rocks come from at least two andesitic and rhyolitic cycles with sedimentary intercalations, all along as a product of the topography and environment of the Permo-Triassic type basin and lakes that favour their deposition between continental cycles [Vergara and Thomas \(1984\)](#); [Bisso et al. \(1998\)](#). [Munchmeyer et al. \(1984\)](#) split the Collahuasi formation into three informal units: La Grande Unit, Capella Unit and Condor Unit.

Quehuita formation Sedimentary rocks defined by [Vergara and Thomas \(1984\)](#) as a marine-continental sequence were deposited on the Collahuasi formation in erosive and angular discordance, defining a lower member and an upper member. The former made up of fangolites, limestones and marine limolites with a Jurassic age with fossils associated with the limestones, and the latter made up of limestones, calcareous sandstones, sandstones and conglomerates.

Cerro Empexa formation Elongated sequence of andesites, dacites and volcanic breccia with intercalations of red sandstones and conglomerates of 95 Ma [Vergara and Thomas \(1984\)](#). It limits to the east with the Domeyko fault system and to the west with the Quehuita formation.

Cenozoic rocks (Ignimbrite) Based on K-Ar in biotite, [Vergara and Thomas \(1984\)](#) defined three bodies of ignimbrites in the northern and eastern part of the Collahuasi district: Ignimbrita Huasco, Ignimbrita Ujina and Ignimbrita Pastillos with 17.1 Ma, 9.3 Ma and 0.75 Ma, respectively. All originated from the stratovolcanoes that currently mark the modern arch. The Huasco ignimbrite has pyroclastic dacitic to rhyolitic sequences associated with eruptions with a lower-middle Miocene caldera collapse, made up of partially or fully welded tuffs. The Ujina ignimbrite corresponds to an upper Miocene deposit made up of welded tuffs and pyroclastic material and occasionally presents flow structures. The ignimbrite Pastillos has a lower member of partially welded tuffs and laharic deposits, and an upper member of unwelded kinetic tuffs with levels of clay, silt and diatomites in the Coposa brine sector.

3.2 Intrusives and mineralization

The intrusive bodies in the Collahuasi district have a composition of diorites, monzonites, granodiorites, and granites ([Munchmeyer et al., 1984](#)). Granites and granodiorites from the Paleozoic pre-continental arc intrude the Collahuasi formation, standing out as a period of emplacement of Permo-Triassic intrusives. A second period with the location of intrusives of quartziferous diorites and granodiorites from the Upper Cretaceous-Lower Tertiary intrudes the Cerro Empexa, Quehuita and Collahuasi formations. A last period, associated with the late Eocene, quartz-monzonite intruded in the Collahuasi Formation, an event related to the mineralization and genesis of the existing porphyry copper deposits ([Munchmeyer et al., 1984](#); [Vergara and Thomas, 1984](#)). Copper mineralization in the Rosario Porphyry is associated with a series of northwest-trending quartz sulphide and massive sulphide veins. Ore-grade mineralization coexist around a biotite porphyritic quartz-monzonite ([Cooke et al., 2005](#); [Masterman et al., 2005, 2004](#)).

Several authors have explored in more details the Rosario Porphyry [Vergara \(1978\)](#); [Munchmeyer et al. \(1984\)](#); [De Beer and Dick \(1994\)](#); [Lee \(1994\)](#); [Clark et al. \(1998\)](#); [Moore and Masterman \(2002\)](#); [Ireland \(2011\)](#); [Dick et al. \(1994\)](#). Mainly, they indicated that the porphyry intrudes the base of the Condor Unit of the Collahuasi formation, showing a southwest fault system, called the Rosario Fault system, which cuts the volcanic rocks and the intrusives of the La Grande and Condor unit. Mineralization and alteration occur at different geological generations and can be grouped into three hydrothermal events: early, intermediate and late [Lee \(1994\)](#); [Dick et al. \(1994\)](#). Nevertheless, the absence of a clear gap between the early and late hydrothermal events suggests that the late burst was generated in a short period of time or that the latter resets the ages of the previous events ([Clark et al., 1998](#)). The [Table 1](#) summarize the information

on the relationship between the different igneous activities and their relationship with the different hydrothermal events regarding mineralization.

4 Background

Contributions made by [Burnham \(1979\)](#) shows the importance of phase separations in the evolution of magmatic and hydrothermal fluids in the formation of copper porphyry. [Sillitoe \(2010\)](#) reviews the relationships between a parental pluton, a multiphase precursor pluton and the formation of porphyry-type ore deposits. Additionally, [Sillitoe \(2010\)](#) exposes the characteristics that in these deposits there are overlays of events (“telescoping”). Additionally, [Sillitoe \(2010\)](#) manifests the presence of overlapping events (*telescoping*) in those deposits. Thus, the formation of porphyry copper has a high participation of magmatic and hydrothermal fluids, making the relationship of fluids and metals in the systems a relevant and key driver of mineralization. One of the best way to obtain a direct information about fluids is by studying the existing fluid inclusions. The fastest, cheapest and most used techniques is by petrographic studies at room temperature ([Roedder, 1984](#)).

4.1 Copper transport and ligands types in magmatic-hydrothermal system

Ideally, the evolution of a magmatic system would be by transcending a hydrothermal system, giving the bases for the enrichment of metal explanation. In this process, the partition is linked to the creation of saline fluids produced by the conjugation of several differentiation and phase separation processes of the magmatic-hydrothermal fluid ([Burnham, 1979](#)). The salinity is measured in equivalent concentrations of sodium chloride. It has been found that felsic magmas are associated with chlorinated ligands for copper, validating that the evolution of the magmatic-hydrothermal transition entails the formation of more saline fluids due to the increase in sodium chloride, helping to evaluate the partitioning and transport of copper under these conditions ([Hedenquist and Lowenstern, 1994](#)).

[Zajacz and Halter \(2009\)](#) studied the ability of copper to be transported as a sulphur complex. They evaluated the effect of several partitions given an vapour exsolution (phase separation) produced in a mafic magma. They postulated that this process, coming from a mafic system, could be mixed with felsic magmas for further copper enrichment. Under these conditions, if we compare the preference of copper to be transported in a liquid phase (chlorinated brine) or a vapour phase (sulphur complex), they found that in the formation of a porphyry copper deposit (i) the transport of chlorinated complex should be an indicator of brines and thus be evidenced in fluid inclusions associated with halite, and (ii) the transport as a sulphide complex, as a gas phase, points to the vapour rich inclusions and/or the presence of opaque minerals in steam inclusions.

4.2 Copper transport in copper porphyry systems: liquid versus vapour

Knowing how copper is transported through complexes, both chlorinated and sulphurized, associated with the brine phase and steam phase respectively. Several authors have evaluated and measured the *partition coefficient* (partition coefficients describe how a solute is distributed between two immiscible solvents) of copper under different condition systems that form porphyry-type ore deposits.

[Williams et al. \(1995\)](#) evaluates this coefficient when copper is transported as a chlorinated complex in the felsic magmas system. Considered the coefficient between the brine-type liquid phase, the vapour phase and the presence of molten silicate type phase, under different pressure and temperature scenarios: between 0.5 to 1.4Kbar and 850 to 750°C. They always obtain a positive value towards the brine vs vapour or molten phase, achieving the highest partition coefficient value towards the brine under the conditions of 1Kbar and 700°C. They concluded that this dependence is directly associated with the chlorine partition between these 3 phases under the conditions of pressure and temperature that were evaluated.

The work by [Zajacz and Halter \(2009\)](#) and [Zajacz et al. \(2011\)](#) are similar to the previous case, with the main difference that they work on the evaluation of the partition coefficient of copper as a sulphur complex under the effect of the phase separation suffered by the melt and which produces brine and gas. They concluded that as sulphur activity increases, copper as a sulphur complex is preferably partitioned to the vapour phase, however, if the sulphur activity is low, the brine phase is highly preferred despite being a sulphur complex. So, the sulphur complex has a direct dependence on the increase or decrease of its partition coefficient with respect to the sulphur activity.

The work by [Frank et al. \(2011\)](#) [Zajacz et al. \(2017\)](#) also explored the previous aspects. They sought to understand the mobility of copper in the systems of synthetic fluid inclusions. They studied the solubility of copper between liquid and gaseous phases considering hydrothermal fluids of different combinations of these salts and gases; NaCl, KCl, HCl, sulphur and others, since the hydrothermal fluids can be defined, studied and understood through the relationship of a

system salts, water and gases. Their results show that the solubility of copper under a NaCl-KCl-H₂O system increases if a little sulphur concentration is added but if HCl is also incorporated, the solubility increases considerably. Moreover, if a joint addition between sulphur and chlorine is considered, the modification of the solubility of copper in liquid or gaseous phases with HCl when adding sulphur is almost nil. It is therefore concluded that copper is further split into aqueous and complex-related solutions chlorinated, depending on the partition of sodium cations and chlorine anions, even if there are abundant cations and low sulphur activity, copper prefers the liquid phase (brine).

Considering the evolution of a first magmatic fluid with intermediate compositions and salinities between 5 and 10 weight percent proposed by the [Burnham \(1979\)](#) model and considering aspects of other authors such as [Bodnar and Beane \(1980\)](#); [Bodnar \(1982, 1995a,b\)](#) or [Cline and Bodnar \(1991\)](#) it is necessary that: the lower part of the system predominates a strong partition from the elements to the liquid phase, in particular of copper, and in the high parts a strong partition of copper to the vapour phase. In this sense, the condensed/separated liquid generates a proportionality to the amount of chlorinated metals formed and this, in turn, controls the field of coexistence between liquid and vapour of the system, retaining copper in the liquid phase.

4.3 Scope of petrography at room temperature of fluid inclusions

The study has been simplified to the consideration of a binary system given by water and salt: H₂O-NaCl. Given this simplification, with the petrography of fluid inclusions at room temperature, considering the rules of [Roedder \(1984\)](#), it is possible to observe the phases present in each inclusion, and even to establish families of fluid inclusions. A priori, the four main phases to consider are: Liquid H₂O, H₂O vapour, Halite crystals and daughter minerals such as chalcopyrite or other opaque as well as translucent silvite type.

[Nash \(1976\)](#) compiles information on the types of fluid inclusions present in porphyric systems and finds a pattern of presence and establishes 4 main types of fluid inclusions associated with these deposits: Rich in liquid (type 1), Rich in vapour (type 2), saturated in Halite (type 3), and rich in CO₂ (type 4), also highlighting the coexistence of liquid and vapour rich inclusions. These 4 types of inclusions are expected to be found in the porphyry copper and can be described petrographically at room temperature by observing the presence of their phases.

[Wahler \(1956\)](#); [Roedder \(1972\)](#); [Bodnar \(1983\)](#), proposed techniques to be used under petrography at room temperature to obtain liquid/vapour ratio values, by the size of the bubble, or salinity values according to a refractive index to know characteristics of the paleofluids without using microthermometry. The relevance of this information, when working with fluid inclusions, is the contribution of data that characterizes the fluid strongly, giving notions of physical and chemical conditions and also mechanical processes such as phase separations in boiling events, under the observation of inclusions rich in liquid coexisting with vapour rich inclusions, as well as high salinities if there are inclusions with halite, and even oversaturated fluids in copper that have achieved be trapped and have precipitated chalcopyrite inside the fluid inclusion ([Roedder, 1984](#)). [Bodnar \(1982, 1983\)](#); [Bodnar et al. \(1985\)](#); [Bodnar and Sterner \(1985\)](#) even proposes a way of giving notions of temperatures and pressures of fluid entrapment, according to the proportion of the liquid and vapour phases of fluid inclusions.

4.4 Fluid inclusions and its relationship with vein types A, B, C, D, E, and TES

The classifications of type of veins are mainly given by the work of [Gustafson and Hunt \(1975\)](#), giving rise to the nomenclature of type A, B and D veins. To this nomenclature, type C veins were added by [Dilles and Einaudi \(1992\)](#), the M-type veins by [Arancibia and Clark \(1996\)](#) and in particular, the work around the Rosario Porphyry, establishes the E-type and late vein stages of tennantite-enargite (TES) ([Masterman et al., 2005](#); [Masterman, 2003](#)). According to [Gustafson and Hunt \(1975\)](#), in the study of the El Salvador porphyry, they conclude that 75 % of copper located in the porphyry is generated in the early stages during potassium alteration along with the mineralization of low sulphur sulphides, associating them with event type A veins. These veins have been observed with fluid inclusions having high salinities and being rich in steam.

[Gustafson and Hunt \(1975\)](#) consider that the intermediate process of the development of a porphyry deposit is when a high sulphuration develops under a strong hydrolytic environment characterized by the location of quartz veins, abundant molybdenite, and tourmaline, characteristics of type B veins. Abundant fluid inclusions of high salinity and rich in gas have been described as type A veins. In some cases, the youngest quartz inside has low salinity inclusions and is rich in liquid.

[Dilles 1992](#) wall found veins different than any intersection of veins type A and B. These mineralogically distinct veins were cut by late-type D. They were established as intermediate veins after type B, named type C. These type C are characterized by having a combination of chalcopyrite, pyrite or bornite, quartz, epidote and chlorite ores, often cut by type D veins from the sericitic alteration. It has been considered that the copper content of the C-veins comes from

removing copper from the A and B types since the internal minerals and the rocks do not leach, leaving the previous alterations/veins as the only source.

According to [Gustafson and Hunt \(1975\)](#) the late event is characterized by abundant mineralization in pyrite and a strong hydrolytic alteration that destroys potassium feldspar and biotite. This produces quartz-pyrite veins, pyrite veins with halos of sericitic alteration, or disseminated pyrite in areas with pervasive sericitization. Under the previous context, type D veins are formed. These are poor in fluid inclusions and have been found to be rich in liquid. It is common to find simple halos of sericitic or sericite-chlorite alteration in small type D veins. When type D veins cut fresh rock in a porphyric environment, these would provide a slight addition to the copper content in that area. While developing over the previous alteration environments and finding themselves cutting the early and intermediate veins, it would fulfill the function of a rework in the copper content of the system.

[Masterman et al. \(2005\)](#) specifies more in the development of late veins and defines type E as massive polymetallic sulphides that cut all other veins except type D veins. While TES type veins are characterized by the presence of tennantite and enargite products mainly to replace the pyrite, bornite, chalcopyrite, and calcosine of type E veins. The exact generalization of what types of fluid inclusions will be found in what type of vein in a copper porphyry hydrothermal system is difficult to determine due to the multiple varieties of processes that these deposits undergo and the same variety in which they occur in the world. Based on all mentioned research, the following highlights are derived:

1. High salinity fluid usually accompanies the deposition of quartz-chalcopyrite in the veins.
2. Generally the economically important mineralization is found in quartz-chalcopyrite and quartz-molybdenum veins which contain only inclusions of moderate salinity.
3. Type 1 inclusions of [Nash \(1976\)](#), are present in all veins, varying only in degrees of salinity.

Frequently, an analysis of fluid inclusions is carried out in copper porphyry investigations when making descriptions of veins. Two case studies are shown to provide some theoretical and practical framework of the process in porphyry copper deposits. The first case study was carried out in El Salvador by [Gustafson and Hunt \(1975\)](#), establishing the types of veins A, B, and D. His observations were as follows:

"Type A and type B veins have inclusions characterized by bubbles of moderate size with the presence of halite and opaque minerals, thought a priori as hematite, rarely there can also be a presence of silvite and on other occasions triangular opaque supposed as chalcopyrite. These inclusions were never observed in type D veins, while high salinity inclusions are highly abundant in type A veins. Fluid inclusions with large bubbles, such that they occupy between 40 and 80 percent of the volume of the inclusion, and that may or may not have small opaque (probably hematite) are found in type A and B veins, but never in type veins D. The inclusions presented in the type D veins are characterized by presenting a small bubble, without the presence of any solid phase, and which, when microthermometry is performed, would represent homogenization temperatures between 175°C to 310°C, while those present in the type A veins and B homogenize at temperature ranges between 360°C and more than 600 °C."

In summary, it can be said that the observations made by [Gustafson and Hunt \(1975\)](#) would be: Type A veins, in El Salvador: High abundance of inclusions of both high salinity and low density (vapour rich). Type B veins in El Salvador: Abundance of inclusions of high salinity and low density, sometimes finding inclusions that tend to be low salinity. Type D veins in El Salvador: Only scattered inclusions of low salinity seen in quartz, anhydrite and sphalerite.

If we transform the observations made on fluid inclusions by them to the classification of the type of fluid inclusions established by [Nash \(1976\)](#), it has that the inclusions described by them as high salinity would correspond to inclusions type 3 fluids, low density as type 2, and low salinity as type 1. Thus, the observations made by [Gustafson and Hunt \(1975\)](#) on the fluid inclusions present in the type of vein in El Salvador, are in line with the types proposed by [Nash \(1976\)](#). Here, the following would be taken:

Type A veins have a high abundance of F.I. rich in gas and saturated in halite (type 2 and 3, respectively). Type B veins have F.I. rich in liquid, rich in gas, and saturated in halite (type 1, 2, and 3, respectively). Type D veins have only F.I. rich in liquid (type 1).

A second case study was carried out by [Masterman \(2003\)](#); [Masterman et al. \(2005\)](#) around the Rosario Porphyry. They identified the types of fluid inclusions trapped in the different types of veins present in the porphyry. Summarizing their descriptions and analysis as: Type A veins present F.I. rich in liquid, rich in steam, and saturated in halite (type 1, 2, and 3). Type B veins present F.I. rich in liquid and rich in steam (type 1 and 2). Type C veins have only F.I. rich in liquid (type 1). Type E veins present F.I. rich in liquid, rich in steam, and saturated in halite (type 1, 2, and 3). Veins of late events of Tennantite-Ennargita (TES) exhibit F.I. rich in liquid (type 1).

4.5 Fluid inclusions and their relationship with the types of alteration

A study carried out on 79 porphyry copper deposits collected information on fluid inclusions associated with hydrothermal alterations present in 13 of these sites, generating a total of 1915 data, plotted after performing fluid microthermometry inclusions [Bodnar et al. \(2014\)](#). In this work it can be seen how fluid inclusions abound more in potassium and phylic alteration than in propylitic and argillic, these last two are grouped in the same box because they are hard to distinguish. In propylitic and argillic alterations, inclusions rich in liquid dominate. The phylic and potassium alterations show a similarity in salinity (0-60 wt percent NaCl) of their inclusions but with a difference in their homogenization temperature, characteristic of the temperature at which these alterations occur.

[Bodnar and Beane \(1980\)](#); [Beane and Bodnar \(1995\)](#) indicate that inclusion type 3, which would be saturated in halite, are present in the potassium alteration, trapped in the early stages when the alteration develops. In turn, type 1, which is rich in liquid, can occur a few kilometers away from alterations of biotite-potassium while type 2, vapour rich, would occur in the porphyry nucleus when they are associated with the potassium alteration.

4.6 Exploration: F.I. and its spatial relationship in copper porphyry and CPPI

A copper deposit can be understood using the binary H₂O-NaCl system ([Burnham, 1979](#)). This allows to schematize the systems due to the petrographically observable characteristics at room temperature of the fluid inclusions extrapolate physical-chemical conditions of the fluid ([Bodnar, 1982](#); [Bodnar et al., 2014](#); [Cline and Bodnar, 1991](#)). Explained in another way; the petrography of fluid inclusions projects spatiotemporal models of the development of a copper porphyry ([Becker et al., 2019](#); [Bodnar, 1982](#)), similar to the known and accepted models of the distribution and temporal development of the alterations of these systems ([Sillitoe, 2010](#); [Singer et al., 2002](#)). [Figure 2](#) represents the fluid inclusions that are used in the schematical distribution.

The latter establishes a copper porphyry probability index (CPPI) based on the relative abundance of the petrographic observations of types of fluid inclusions present in a sample, relating the importance of inclusions with halite due to the influence of the presence of chlorine for generating copper transports as chlorinated complexes ([Bodnar, 1982](#); [Roedder, 1997](#)). This index can be used for exploratory purposes because it generates a spatial notion of being in the presence of the boundary between the potassium and phylic alteration of a porphyric system. This border in many copper porphyry deposits in the southwestern United States would be the copper mineralization zone ([Beane and Bodnar, 1995](#); [Bodnar, 1995a,b](#); [Singer et al., 2002](#)). It must be said that the index established by [Bodnar \(1982\)](#) used in isolation is inconclusive since these fluid inclusions saturated in halite and rich in vapour, can be found in other geological contexts. An example of this would be represented by epizonal intrusions mineralized. However, the presence of chalcopyrite as a daughter mineral at least is an indicator that the fluids transported and mineralized copper.

The previously mentioned spatiotemporal schematization model establishes an initial compositional characteristic of hydrothermal fluids. Then, vertical patterns and temporary distributions of inclusions with specific features, and how they can be used to vectorize the peripheric and central areas of a copper porphyry and also where important mineralization usually occurs, are concluded. [Figure 2](#) shows an illustration, description, and location of fluid inclusions considered by the aforementioned studies, in particular, the schematic graph of [Bodnar \(1982\)](#).

5 Case of study

Data collection. We work with 268 quick plates, which represent 268 points in space obtained from exploration drill holes. The quick plates were prepared in the cutting laboratory of the University of Chile, approximately with a thickness between 80 and 100 microns, which are coated with an immersion oil with the same index of reflection as the quartz to facilitate observations of fluid inclusions trapped in this mineral. It was sought to observe in each of them the presence of 7 types of fluid inclusion (FI) assembly characterized by phases present at room temperature, shown in [Figure 3](#).

The code used is (a) Type 0: FI liquid rich, (b) Type 1: FI halite bearing, (c) Type 2: FI with opaque minerals daughter, (d) Type 3: FI with chalcopyrite daughter, (e) Type 4: coexistence of FI vapour and halite with or without chalcopyrite, (f) Type 5: coexistence of FI vapour and liquid rich, (g) Type 6: FI vapour rich.

In addition, observations are made to quantify the relative abundance of inclusions rich in vapour, inclusions with halite, and inclusions with chalcopyrite, in order to be able to assign to each quick plate, sample, a CPPI value ([Bodnar, 1982](#); [Roedder, 1997](#)). This assignment is made by a percentage criterion of the observer, as well as the allocation of the amount of quartz in a thin section or a hand sample. When was difficult to assign, modal counts were used, to give notions of relative abundance between each type of inclusion.

6 Results

6.1 Petrographic observations of fluid inclusions at room temperature.

We worked with 300 rocks used as representative specimens of a volume of area related to the environment of the copper Porphyry Rosario. These rocks are samples of drill holes. Of the 300, 277 quick plates were obtained (1 per specimen), with 23 samples remaining outside the case study. At 277, petrography was carried out that sought to explain whether or not it presented the pre-established fluid inclusion family, defined in the methodology, assigning a value of 1 or 0 to the sample and whether or not it presented the type of fluid inclusion family. Almost all of the FIAs observed corresponded to secondary fluid inclusions, so a distinction of the primary inclusions is not made, and for the convenience of the reader, we can recommend that they assume all as secondary, although it is not the main approach considered in this work. It is recalled that all inclusions were observed in the quartz veins.

The [Table 2](#) indicates the number of samples that have at least that type of inclusion sought. This table shows the predominance of liquid rich inclusions, followed by vapour rich, and thirdly evidence of the coexistence of liquid rich with vapour rich inclusions, followed by saturated halite inclusions. The CPPI assessment and his value assignment were performed on each sample. Remember that this parameter is not linked to a family of fluid inclusions, but to the existence, and abundance, of the 3 types established by [Bodnar \(1982\)](#). Beheaded inclusions are not used the whole study.

The histogram ([Figure 4](#) left) is created based on obtained values by petrography observation of CPPI to find a concentration tendency in some value or value range. Has 6 classes, separated by 4 units of CPPI value each and considering 0 as information of an individual class. It can be seen that the range of 5 to 8 is the most predominant, then the lowest classes dominate over the highest. The minimum value was 0 and the maximum 14, and the latter was reached in only 2 samples. Important: There are no samples that reach values over 14.

6.2 Petrographic observations of veins

The rock could present a single type of veins, or a crossing of these, or both situations. The abundance indicates the number of samples in which they were observed with that type of vein ([Figure 4](#) right). Predominates the presence of type D veins, followed by types E and then type B.

If grouped sampled that present type B veins, D and/or crossing of these (BD) would have a total of 135 (31 + 66 + 38). This is important if we consider that these types of veins are responsible for the contribution and/or remobilization of copper in copper porphyry ([Gustafson and Hunt, 1975](#); [Sillitoe, 2010](#)). The rocks with quartz veins that represented a propylitic alteration ("vt Prop") and the rocks with quartz veins in samples with evident degrees of leaching, could be grouped as veins associated with alteration (are indicated how alteration vein) and would correspond to 40 (24 + 16). In the same way, all samples with crossings of veins, indicated as crossed veins, can be grouped into a single class, and these would correspond to an amount of 50 (5 + 3 + 38 + 4).

Type D veins are predominate, followed by cross veins, where in these later the constant participation of type D veins stands out, thirdly type E veins and fourthly type B. Given the above, the presence of late veins, especially type D, stands out, with a total participation of 116 (66 + 5 + 3 + 38 + 4), corresponding to 42 percent. Then in percentage is continued by type E veins, 16.6 percent, followed by type B veins with 11.2 percent.

6.3 Relationship between type of fluid inclusions and vein vs depth, 1D

The relationship with a first spatial dimension is worked on, which in this case has been considered the depth measured as meters above sea level (m asl) that corresponds to the position of the sample at the time of having been obtained by drill-hole. With this, the first indications of some relevant or important distribution can be given in the vertical volume characterized by the samples studied. For this, separate figures are created from each type of inclusion and, each type of vein in their general grouping (individual, cross, alteration).

The depth levels range from 4600 to 3500, so a level is established that divides the sector into a deep area by being below it. This level is 3800m asl. allowing us to consider 300 meters as long of the deepest sector of the study area, which would correspond to 27.7 percent of the vertical. To decide this level, it is considered that around 3800 (m asl) the distribution of the samples presents jumps, gaps, and important variations, and this allows it to be considered as a relevant level in the behavior of the parameters evaluated.

An example of this is the distribution of inclusions becoming less abundant or continuous, and in particular distributions of types of veins stand out as gaps and discontinuity or non-continuity for types A, C, D, E, TES, Cross, and Alteration,

while type B veins don't show presence between 3900-3800 m.a.s.l., but under 3800 shows great continuity and abundance. So it is named as a deep level, under 3800 m.a.s.l.

With the previous division of the sector, distribution characteristics can be established in the deep zone vs the shallow zone (under or over 3800). Observing a homogeneous distribution, without variation, throughout the vertical in the follow fluid inclusions: liquid rich (type 0, Figure 5.b), saturated in halite (type 1, Figure 5.c), and inclusions that show boiling due to the presence of coexistence of inclusions liquid rich and vapour rich (type 5, Figure 5.g). It can be said that the whole sector has evidence of boiling and witnessed such an event. However, not all vertical presents a fluid with chalcopyrite saturation (type 2, Figure 5.d) or boiling with brine formation (type 4, Figure 5.f). The vertical distribution of fluid inclusions with chalcopyrite as a daughter mineral inside (type 2, Figure 5.d), show a marked discontinuity in shallow areas in the depth ranges of 4,500 to 4,300 m.a.s.l. The coexistence inclusions between the vapour phase and brine (type 5, Figure 5.g) have a gap between 3700 and 3550 m.a.s.l. (150m). Under 3700 there is no evidence of vapour-rich inclusions (type 6, Figure 5.h).

At 3700 there is the latest evidence of fluid inclusions with chalcopyrite, then there is evidence of inclusions with metals that cannot be distinguished whether or not they correspond to chalcopyrite (type 3, Figure 5.e).

Then, between 3700 and 3550, there are only inclusions rich in liquid and, coexistence of rich vapour and rich liquid. Be interpreted as a phase separation zone without causing saturation-precipitation.

Type A veins (Figure 6.a) are preferentially 200 meters below the surface, covering an area of 300 meters (4,450 - 4,200 m.a.s.l.) and then present about 150 meters in depth another small event of veins type A and another at 3850 m.a.s.l. These two possible zones of depth, one more shallow than the other, may be indicating the early temporality of two different events produced at different depths. Similarly, it is observed type B veins (Figure 6.b) with a more homogeneous vertical distribution but which can also be grouped into two main areas, one more superficial and one deeper, separated between 3,950 - 3,800 masl. This distribution of superficial and deep zones can also be visualized in the type C, E and alteration veins (Figure 6. c, e,h), while the type D veins (Figure 6.d) show a distribution mainly present in the shallow zone, as well as the crossed veins (Figure 6.g). The TES veins (Figure 6.f) present are few and only on the shallow level.

Therefore, in the shallow area early and late veins predominate. There is an area in the deep zone, under 3700 to 3500 m.a.s.l., where there are only type B veins, with fluid inclusions that; they show boiling (type 5, Figure 6.g), presence of opaque metals such as chalcopyrite (type 4, Figure 6.f) and halite saturation.

6.4 CPPI value distribution in depth

A correlation between the depth - CPPI relationship is highlighted, where at shallower, less deep levels, the values are dominated by the lowest. It is possible to find in samples at greater depths CPPI values of 5 or more, however there is no clear trend of whether: "As deepens increases the value". Furthermore, there are no samples in the deep zone with extreme values, either low or high. A curious observation could be given by the fact that the extreme values, both low and high, of CPPI are usually distributed at medium depths, close to 4,000 m.a.s.l. (Figure 7) therefore, it is possible to question the role of importance in lateral variation (horizontal, X and Y axes in the Cartesian system) and not only vertical direction (Cartesian Z axis, seen in m.a.s.l.).

6.5 Types of veins according to the CPPI intervals

Generated with the objective of counting the amount of repetition of a type of vein present in the sample associated with the CPPI value ranges, the obtained is illustrated as a bar graph that resembles a histogram, shown in figure Figure 8, where it can be seen that at CPPI values greater than 8 dominate type B, D and combined veins. The latter dominate mainly because the combination is usually given by cross-linking of type B and D veins (cross vein type B-D). Type A veins are present in equal measure for the 3 dominant intervals of the CPPI values, making them a characteristic independent of the CPPI value.

The late veins type TES (tenantite-enargita-stage) are showing to be synonymous with low probability of copper porphyry in the sector where they are present, while the E, are an indicator of an area with intermediate probability of copper porphyry, however type D and mainly type B veins indicate an area of good probability to find a richly mineralized copper porphyry, in accordance with the postulates that type B veins and type D veins are associated with the contribution, precipitation of work and / or remobilization of the pre-existing copper

6.6 Distribution of relevant fluid inclusions, associated with veins, in depth: Schematic temporal-space representation of types of vein and fluid inclusions

Considering the temporal knowledge of the types of veins that are present in the porphyry type deposits according to their relationship with the formation of these and already having observed how each of these are distributed vertically, it is considered to see how present and distribute fluid inclusions in types of veins. It will work with samples that present a single type of veins and have at least the following fluid inclusions: FI with chalcopyrite or possible chalcopyrite (type 2 and 3, Author), inclusions that represent phase coexistence (type 5 and type 4, Author).

The graphs presented in [Figure 9](#) allows to generate an idea about the evolutionary temporality of fluids. If we remember that the B-vein develop first than the D-type veins, an overlap of the latter is expected in the places where the B-type veins occur, or that the D-type veins are at more superficial levels with respect to the veins type B as a succession of the temporal process that generates the vein sequence of the porphyry.

In both upper figures ([Figure 9](#)) it can be seen how the deep zone, under 3,800 m asl, is characterized by type B veins which in turn illustrate phase coexistence events both gas phase coexisting with liquid phase or vapour phase coexisting with brine. These same conditions have over 3,800 m s.n.m. but this time also with the presence of type D veins that suffered similar processes and conditions. As there is no detailed study on the composition of the fluid that is present in each vein, one cannot speak of different fluids between one sample and another. It can only be established that these conditions are present in two stages of the formation of the copper porphyry (intermediate stages represented by type B and late stages represented by type D veins). The interesting thing is how, from the 2 lower graph's [Figure 9](#), the deep zone is also characterized by this coexistence of phases, steam and brine, but it also has the characteristic of presenting a saturated fluid in possibly chalcopyrite evidenced by the presence of fluid inclusions type 3 and inclusion type 4 with chalcopyrite included.

By asking the following questions: If the fluids that took place under 3,800 originate are those that rise, evolve and are present in type D veins; Why do you have type B veins in the upper area? Or if type D veins are developed in the same sector from the same fluid that evolves and is present in type B veins (emphasizing the area over 3,800 m asl), Why do these conditions exist in fluids in type B vein in depth?. It is noted that more information is needed to spin the fluid evolution more rigorously, but if or if you can talk about different events and it is not illogical to think that the area under 3,800 is either a younger event or an event later, but being a later event it would be indicating that the type B veins in the upper area are younger and does not seem logical. The error of this logic is that a fluid would be needed that generates an overlap of events in said area (shallow zone) but that has not generated any modification in the deep zone. But if the youngest deep type B veins are considered, it is acceptable that type D veins abound in the upper area, and if or if it would mean that there are D veins of different temporalities. This would support why there are 1 to 2 of these samples under 3,800.

6.7 Fluid inclusions and CPPI values, in profile.

To construct the diagram temporal-space distribution of fluid inclusions expoused at literature, is considered fluid inclusion that represent boiling, salinity and metal concentration (illustrated in [Figure 2](#)). For this we remember that the fluid inclusions that show boiling are those that in this work are defined as type 5 and 6. Similarly, the fluid inclusions that have chalcopyrite are type 2 and possible 3. The fluid inclusions with halite, coexisting or not with inclusions rich in steam are types 1 and 4 (see [Figure 3](#)).

Joining the distribution of fluid inclusions to the lithological profiles of the Rosario porphyry area, [Figure 10](#) and [Figure 11](#), profiles AA' and BB' are obtained. From these figures, there is a marked distribution of fluid inclusions with halite, chalcopyrite with or without vapour-rich inclusions, in the lithological areas of the Rosario porphyry, that is, these inclusions would be associated with the presence of the Rosario porphyry in its most central zone, noted in particular in the DDH110 and DDHR097 drill-hole of profile AA' and BB' respectively. Comparing the fluid inclusions present in the drill-holes and the spatial distribution of these, it can be established that boiling is a dominant characteristic and that it is presented throughout the profile of both AA' and BB', however, certain areas are established where this boiling is more abundant, for example: The difference in abundance between C167 versus DDH110 in [Figure 10](#).

Spinning more detailed in the distribution of the types of fluid inclusions along the drillholes, it is emphasized that saturated inclusions in halite and copper are more discrete and less abundant, presenting themselves throughout them in specific areas, however, when there is a presence of inclusions with chalcopyrite, it is common to find around them, or together, inclusions also with halite, chalcopyrite with or without the presence of vapour rich inclusions. This observation does not apply to DDHR229 probing.

The structures in both profiles show an influential factor in the presence of fluid inclusions, with a higher concentration (of these three graphic ways of grouping the 7 types of inclusions, defined in this study) in the direction of the failures,

both for the failure Ultima Fault, Pique Fault and Rosario Fault System. And following with the observations on directional distribution of inclusions, we can see in the profile BB' a tendency of distribution in the southwest direction of inclusions with halite, chalcopyrite with or without vapour rich inclusions, which would be a deepening of these in parallel direction to the Pique Rama Fault.

Similar to the previous point, the distribution of the copper porphyry probability index (CPPI) values with respect to the AA' and BB' profiles, presented in value ranges: 0-2; 2-4; 4-6; 6-8; 8-10 or more.

This establishes a direct relationship between the lithological zones of the Rosario porphyry and the high values of the probability index of the copper porphyry, being an observation in favor of the function that the latter fulfills as a probabilistic indicator of important mineralization since the greater it should be indicating greater probability of presence of porphyric system. This is true in both profiles and, in turn, it is appreciated that these values may be correlated to places with structures, presenting in the vicinity of the mapped areas with profile faults. The hypothesis of a correlation with the direction of their propagation is posed. The latter is well observable in the DDHR222, DDHR241 of the AA' profile and the DDHR097 of the BB' drillhole (Figure 12 and Figure 13 respectively), where the samples with high values are very close to the structures. In Profile AA' (Figure 12) it is observed that the DDH502 and the upper area of the DDHR222 probe have very low CPPI values, being remote places in relation to the location of the lithology Rosario porphyry within the profile apart from being more shallow areas in NE and SW direction.

The distribution of intermediate values obtained in the present study, would be given by the interval from 2 to 8. In Profile BB' (Figure 13) a characteristic spatial distribution of lower to higher value of this interval is shown from the upper part towards the deeper part of the profile, in particular the higher values in the SW direction are deepened, direction represented by the arrow. This address is parallel to the prolongation of the Pique, Pique Rama and Rosario System faults, and in turn said location is characterized by being a sector with lithology.

7 Discussion

7.1 Schematic temporal-space representation of types of veins and fluid inclusions

Ideas about the evolutionary temporality of fluids can be generated with these associations. If we remember that the B-vein develop first than the D-type veins, an overlap of the latter is expected in the places where the B-type veins occur, or that the D-type veins are at more superficial levels with respect to the veins type B as an effect of the rise of fluids and the temporal process that generates a sequence of veins in the porphyry.

As there is no detailed study on the composition of the fluid that is present in each veins, one cannot speak of different fluids between one sample and another. It can only be established that these conditions are present in two stages of the formation of the copper porphyry (intermediate stages represented by type B veins and late stages represented by type D veins).

By asking the following questions: If the fluids that took place under 3,800 are the ones that rise, evolve and are present in type D veins, why do you have type B veins in the upper area? Or if type D veins are developed in the same sector from the same fluid that evolves and is present in type B veins (emphasizing the area over 3,800 masl). Why do these conditions generate type B veins in deep? It is noted that more information is needed to spin the fluid evolution more rigorously, but yes or yes you can talk about different events and it is not illogical to think that the area under 3,800 is either a younger event or an event later, but being a later event it would be indicating that the type B veins in the upper area are younger and does not seem logical.

The error of this logic is that a fluid would be needed that generates an overlap of events in said area (high zone), but that has not generated any modification in the deep zone. But if the youngest deep type B veins are considered, it is acceptable that type D veins abound in the upper area, and if or if it would mean that there are D veins of different temporalities. This would support why there are 2 of these samples (D-vein) under 3,800.

It should be noted that geological systems are dynamic and it is an assumption to consider a direct vertical rise of the fluid. That is, the deep and shallow zone are connected in the system to rule out the possibility that the upper zone with veinlets B are not younger. In other words, a curved-lateral migration of more distant fluids, due to fractures and other factors, could be another scenario to be evaluated and a vertical passage of the same fluid formed is assumed.

We assume the directionality of the rise with the trend of the structures of the profiles. We also leave in evidence how important it is to have a scenario, model, clear of the evolution of the system so that the F.I. when used as a tool they take more force.

7.2 Comparison between theory and application of real data

Based on what was stated by [Gustafson and Hunt \(1975\)](#), [Nash \(1976\)](#), [Roedder \(1972, 1984, 1990, 1997\)](#), [Bodnar \(1982, 1995b\)](#); [Bodnar et al. \(2014\)](#), [Singer et al. \(2002\)](#), [Masterman et al. \(2005\)](#), [Yardley and Bodnar \(2014\)](#), and other much authors referenced around fluid inclusions and copper porphyry, a correlation can be made between the theory and what is observed in the Rosario copper porphyry with respect to the presence of fluid inclusions.

They proposed that the presence of liquid rich fluid inclusions (low salinity) were present in all types of vein and distributed throughout the system area, which is corroborated in this study with the almost omnipresence of liquid rich inclusions (type 0, Author) in the samples. Similarly, in the system there is a wide presence of liquid rich and vapour rich fluid inclusions coexistence (type 5, Author). This is a situation that has been theoretically proposed as a characteristic of copper porphyry and is revalidated. In the case of inclusions with halite or chalcopyrite, these are more selective in their distribution and their manifestation varies, but they make reference to the need for the presence of saline fluids (brine) and with appreciable copper concentrations that took place in the development of the copper porphyry, fluids that tend to indicate: “presence of copper mineralization” [Bodnar \(1982\)](#); [Roedder \(1997\)](#).

If the graphs from figure 4.a to 4.g on the distributions of the IFs are observed, they exhibit certain discontinuities and show their specific spatial distribution in the vertical. This indicates levels at which fluid paleo experienced specific processes, either phase separations or element enrichments, characterizing the fluid at that level. And if you consider the figures of the distribution of veins (from Figure 5.a to 5.h), these also manifest particular conditions at specific levels, such as, the presence of veins type B (intermediate temporality) in depth with types of early veins (type A or AB transition) and not so late veins in depth. If this is added to the fact that deep inclusions of high salinity can be found in depth (type 1, 3, 4 and 5, Author), and is analyzed remembering that the potassium alteration is characterized by veins type A, B and AB, as well as for fluid inclusions that can reach salinity of up to 60percent wt NaCl and for fluid inclusions that could represent boiling, it is possible that the deep Rosario porphyry rocks represent a zone of potassium alteration with paleo fluids that experienced boiling and partition of elements, so it is considered an economically important copper mineralization zone.

To address this last consideration, [Figure 12](#) and [Figure 13](#), where the spatial distribution in area profiles, AA' and BB', of the copper porphyry probability index (CPPI) values can be used. Remember that this index indicates probability of economic mineralization in a copper system linked mainly to the area between potassium and phylic alteration ([Roedder, 1997](#)). With the distribution of CPPI in both profiles we can see a growth in their values in depth and with a direction to the southwest, place that has originated the hypotheses proposed by [Masterman \(2003\)](#); [Masterman et al. \(2005\)](#); [Cooke et al. \(2005\)](#), which supports the relevance of this sector as an important zone of copper mineralization. It should be noted that these profiles have high values (within the results of the study) often associated with the profile structures, which could be indicating the favorable way of transporting fluids with salinities and concentrations of important metals due to phase separations suffered at greater depth.

If we consider that we are in the presence of a copper porphyry and that the CPPI is based on being in front of samples of these systems, results of assigning values in the samples between 0 to 22 should be obtained, as originally proposed, however, the investigation assigns to the 277 samples a range of value between 0 to 14 of CPPI, observable in [Figure 4](#). This may be due to various reasons: one of them is that the samples that could reach higher value in the site, were not taken or studied. Another reason may be the inexperience of the one who performs the petrography of fluid inclusions to establish a quantification of the presence of the types of inclusions or perhaps only the reserved way of assigning quantitative values, moderating to almost 50percent the allocation of scale value. The relevant thing is that since all values are assigned by the same person, although their criteria and experience may influence, the pattern of low values and high values can still be usable under the concepts of utility proposed by [Bodnar](#), that is, the case study qualifies for its CPPI values to be usable by having a wide, measured range, but which allows discretization in areas of low, medium and high value, and exceeding the average value of the original scale.

Accepting that there is an area in the southwestern direction relevant in matters of mineralization, indicated by the distribution of fluid inclusions, veins, CPPI value and supported by sector profiles, the possibility of fluid inclusions to perform exploration would be corroborated, because they would validate and indicate the “important mineralization” zone.

To establish a higher understanding such that they can solve the hypotheses raised, a more detailed use of the results obtained must be made; therefore there are 10 samples presented in [Figure 14](#), where each sample is represented by its most abundant, characteristic fluid inclusion type.

Considering the two series established in figure [Figure 14](#), we can say that there are two levels where a phase separation (immiscibility) is generated that can be associated with the same fluid or two different fluids with their corresponding series (one fluid for each series). These levels are represented by samples NA-7(#3) and DM-14(#9), see [Table 3](#). This separation of the fluid generates a high salinity phase with metal saturation (chalcopyrite in the case of the DM-14

sample) and a vapour phase. The abundance of chalcopyrite, halite and their sizes in the DM-14 sample compared to the NA-7 sample, in which the precipitated metals are small and difficult to identify, would be evidencing separate events of immiscibility, so consider them as different fluids is relevant. In addition, this observation is supported by the descriptions of the samples where the presence of other fluid inclusions is not correlative, indicating that these rocks were not under the same event, although the fluid that circulated on them underwent a very similar process. This together with the difference of the vertical sequence of the inclusions of each series would be an indicator to refute the hypothesis of a deep zone due to a structural displacement of the Rosario porphyry proposed by (Masterman et al., 2005; Cooke et al., 2005).

Now to obtain answers to the other 2 scenarios planted by the remaining hypotheses by Masterman et al. (2005), figure Figure 15 based in the schematic figure proposed by Bodnar (1982); Becker et al. (2019); Klyukin et al. (2019) must be used. If we consider that the series simply represent a vertical surface-to-depth graph of a porphyry system, without considering the temporality of its development, that is, they are all inclusions of a young or old porphyry. Only the lower part of the Figure 15, stage 1 for series 1 and stage 2 of series 2 presented are obtained. This results in the non-similarity sequences, indicating to consider each sector as distinct porphyric systems, which would be supporting the hypothesis of being a deeper intrusive separated and younger than the porphyry Rosario, associated perhaps with him in terms of source but not in developing.

If we consider that everything develops at the same age, fixed time, we must use both parts of the graph proposed by (Bodnar, 1982) in Figure 15, where we would be placing the series 1 as a central area with slight displacement to the periphery, which would come to be represented by upper part of stage 3 of figure Figure 15. Leaving time fixed and considering that the series 2 should represent a deeper zone (if it was not displaced by faults, Figure 16 can be use it too) it would have to be found if or if in stage 3 set out in the lower part of Figure 15, this would imply that it should be dominated by rich inclusions in vapour with precipitation of chalcopyrite together with inclusions rich in halite with chalcopyrite coexisting with fluid inclusions rich in vapour, however we remember that this series contains an interval of almost 200 meters where the dominant inclusions are of the type rich in liquid (type 0, Author. Figure 5), which would not be represented in stage 3, and in case of considering raising and/or decreasing the depth that would represent the series 2 the upper part would be lost with inclusions rich in vapour. The latter would be refuting the hypothesis of continuity of the system in depth, since a correct correlation of fluid inclusions is not seen, and it supports with greater certainty the hypothesis of a slightly younger secondary intrusive and with copper mineralization in depth (Figure 16).

The different percentage of salinity would be correlated with different pressure measurements, which would correspond to different isotherms. Sample number 9 (Table 3), which is currently in deeper zones of the study area, has higher salinity than sample 3. If both samples were under the same hydrothermal process that developed mineralization and then there was a displacement, then the samples were not they were at the same paleo-level because they developed different percentages of salinities under the same isotherm. In that case, series 2 would represent the most superficial part of the system and series 1 the deep zone. If the hydrothermal processes happened syn or post deformation, then the only way for the series 2 to represent with its sample number 9 a deeper location is that each belongs to different isotherms. Having 600C for sample 9 and 500 for sample 3.

Therefore, the difference between halite and chalcopyrite sizes of the inclusions that show the immiscibility of samples 3 and 9 is very relevant. With this it can be quickly deduced that in the first instance they do not belong to the same paleo-level, and can be that, they do not represent the same hydrothermal flow, process, that they were subjected to if the temporality of structural events is considered. So, is important to know what was first.

Stage 3 of Figure 15 that exposes that everything develops at the same time, lacks congruence with the fluid inclusions observed in the series, since it does not manage to coincide the ends of inclusions rich in steam in the upper part with the inclusions rich in liquid as lower part of the system or steam rich both upper and lower part (that is, if: the vertical sequence developed before or after deformation would be series 1-2 or series 2-1, from top to bottom). While stage 1 and 2, which represent separate situations, different systems, for each series, correlate to a greater extent or similarity with the spatio-temporal distribution proposed by (Bodnar, 1982). In this case, Figure 16 should be studied from the perspective of two different isotherms. So it is important to know the isotherm that the samples would represent, either due to mineral association or alteration or vein. In this case, both samples present the same alteration, but sample 9 has B type vein and sample 3 D type vein. So, the evolution of the same process is incongruous because we have that the elevated part is later (vein d) than the deep part (vein b), and the evolution of a system is from the bottom up, so that an overlapping of late processes in the deep part. If more accept. it is more acceptable that it be another system with another temporality towards the depths of the SW sector.

8 Conclusion

The use of several parameters complemented each other helps to reduce uncertainties, the quantification of this level of reduction would be an interesting study to be carried out to see the degree of impact that is had when conducting exploration by adding information of fluid inclusions, or seen in another way, adding information of mineralizing fluids. Following this complementation between parameters; not complementing the CPPI and working in a single dimension, it does not grant the same clarity of information as if it is worked in 2 dimensions and in conjunction with other research variables. Working the CPPI alone but in 2D allows and delivers high and easy characterizations and/or correlations of the sector, more if it is worked on profiles. The resulting 2D sections can serve as master sections for implicit modeling.

In the same way, the utility of observing the distribution of types of inclusions associated with types of veins allows to strongly characterize the studied area in a single dimension. Represent levels and sectors of mechanisms such as boiling, phase separation, brine and fluid formation with supersaturation of metals, and temporality of events when associated with the temporality of the veins.

Being able to establish the composition of the fluids, and the temporality by assigning if the inclusions observed are primary and/or secondary and in what type of veins were observed, it would be able to give greater clarity to the evolution of the system. However also with only the usefulness of reasons and proportions of the phases present in fluid inclusions and the spatial location of the sample in which the samples were observed, allow a study on pressure and temperature to be carried out, using the Pressure vs. Salinity graph, supported by [Bodnar \(2003\)](#), [Klyukin et al. \(2019\)](#), and [Becker et al. \(2019\)](#). This gives preliminary notions of the evolution of the system.

With this study, you can give the first indications about the use and how you can characterize a study volume. Note that the use of the CPPI values is not simple. Being an observation that fulfills a function as a probabilistic indicator of important mineralization, but therefore it is necessary to establish a practical and accurate methodology to obtain a standardization in obtaining the values assigned to the samples based on the abundance of the 3 types of established fluid inclusions. In this way, it would be used more robustly by other researchers and would facilitate comparison between studies that apply it, to refine. Here it is proposed that a percentage allocation or modal count be used, indicating which method will be used, and by what form.

Finally, the present work highlights the potential of deeper copper mineralization linked to a porphyry system different from the Rosario Porphyry, but both connected to each other. Similarly, a response to the hypotheses proposed by ([Masterman, 2003](#); [Masterman et al., 2005](#)) on the possible copper mineralization in-depth southwest of the Rosario Porphyry is postulated by only the use of room temperature petrography of fluid inclusions.

It is worth mentioning that the only way to achieve complete certainty of the potential of fluid inclusions as an exploration method of copper porphyry is to find the mineralized porphyry based on the use of the method, suggesting that those who work with it can report such results to refine the exploratory technique.

Acknowledgements

Authors would like to thank the support and guidance of Dr. Daniel Moncada, from Universidad de Chile.

Conflicts of interest

The authors declare no conflict of interest.

Nomenclature

The following abbreviations are used in this manuscript:

FI Fluid inclusions
CPPI Copper porphyry probability index
FIA's Fluid inclusion assemblages

References

Arancibia ON, Clark AH (1996) Early magnetite-amphibole-plagioclase alteration-mineralization in the island copper porphyry copper-gold-molybdenum deposit, british columbia. *Economic Geology* 91(2):402–438

- Beane R, Bodnar R (1995) Hydrothermal fluids and hydrothermal alteration in porphyry copper deposits: Arizona geological society digest 20
- Becker S, Bodnar R, Reynolds T (2019) Temporal and spatial variations in characteristics of fluid inclusions in epizonal magmatic-hydrothermal systems: Applications in exploration for porphyry copper deposits. *Journal of Geochemical Exploration* 204:240–255
- Bisso C, Duran M, Gonzales A (1998) Geology of the ujina and rosario copper porphyry deposits collahuasi district, chile. *Porphyry and Hydrothermal Copper and Gold Deposits: A Global Perspective* PGC Publishing, Adelaide pp 217–232
- Bodnar R (1982) Fluid inclusions in porphyry-type deposits. Course notes, Miner Deposits Res Rev Ind, P State Univ
- Bodnar R (1983) A method of calculating fluid inclusion volumes based on vapor bubble diameters and pvtx properties of inclusion fluids. *Economic Geology* 78(3):535–542
- Bodnar R (1995a) Experimental determination of the pvtx properties of aqueous solutions at elevated temperatures and pressures using synthetic fluid inclusions: H₂O-naCl as an example. *Pure and applied chemistry* 67(6):873–880
- Bodnar R (1995b) Fluid-inclusion evidence for a magmatic source for metals in porphyry copper deposits. *Mineral* 23:139–152
- Bodnar R, Beane R (1980) Temporal and spatial variations in hydrothermal fluid characteristics during vein filling in preore cover overlying deeply buried porphyry copper-type mineralization at red mountain, arizona. *Economic Geology* 75(6):876–893
- Bodnar R, Sterner S (1985) Synthetic fluid inclusions in natural quartz. ii. application to pvt studies. *Geochimica et Cosmochimica Acta* 49(9):1855–1859
- Bodnar R, Burnham C, Sterner S (1985) Synthetic fluid inclusions in natural quartz. iii. determination of phase equilibrium properties in the system h₂o-naCl to 1000 c and 1500 bars. *Geochimica et Cosmochimica Acta* 49(9):1861–1873
- Bodnar R, Lecumberri-Sanchez P, Moncada D, Steele-MacInnis M (2014) 13.5—Fluid inclusions in hydrothermal ore deposits. *Treatise on Geochemistry, Second Edition* 10th edn Elsevier, Oxford pp 119–142
- Bodnar RJ (2003) Introduction to aqueous-electrolyte fluid inclusions. *Fluid inclusions: Analysis and interpretation* 32:81–100
- Burnham CW (1979) Magmas and hydrothermal fluids. *Geochemistry of Hydrothermal Ore Deposits* pp 71–136
- Camus F (2002) The andean porphyry systems. *Giant ore deposits: characteristics, genesis and exploration CODES Special Publication* 4:5–22
- Clark AH, Archibald DA, Lee AW, Farrar E, Hodgson CJ (1998) Laser probe ⁴⁰Ar/³⁹Ar ages of early-and late-stage alteration assemblages, rosario porphyry copper-molybdenum deposit, collahuasi district, i region, chile. *Economic Geology* 93(3):326–337
- Cline JS, Bodnar RJ (1991) Can economic porphyry copper mineralization be generated by a typical calc-alkaline melt? *Journal of Geophysical Research: Solid Earth* 96(B5):8113–8126
- Cooke DR, Masterman GJ, Berry RF, Walshe JL (2005) The rosario porphyry cu-mo deposit, northern chile: Hypogene upgrading during gravitational collapse of the domeyko cordillera. In: *Mineral Deposit Research: Meeting the Global Challenge*, Springer, pp 365–368
- De Beer LJ, Dick LA (1994) Development of the collahuasi copper deposits—a world-class copper project in the andes of northern chile. In: *Mining Latin America/Minería Latinoamericana*, Springer, pp 181–195
- Dick L, Chavez W, Gonzales A, Bisso C (1994) Geologic setting and mineralogy of the cu-ag-(as) rosario vein system, collahuasi district, chile. *Society of Economic Geologists Newsletter* 19:6–11
- Dilles JH, Einaudi MT (1992) Wall-rock alteration and hydrothermal flow paths about the ann-mason porphyry copper deposit, nevada; a 6-km vertical reconstruction. *Economic Geology* 87(8):1963–2001
- Frank MR, Simon AC, Pettko T, Candela PA, Piccoli PM (2011) Gold and copper partitioning in magmatic-hydrothermal systems at 800 c and 100 mpa. *Geochimica et Cosmochimica Acta* 75(9):2470–2482
- Goldstein RH, Samson I (2003) Petrographic analysis of fluid inclusions. *Fluid inclusions: Analysis and interpretation* 32:9–53
- Gustafson LB, Hunt JP (1975) The porphyry copper deposit at el salvador, chile. *Economic Geology* 70(5):857–912
- Hedenquist JW, Lowenstern JB (1994) The role of magmas in the formation of hydrothermal ore deposits. *Nature* 370(6490):519

- Ireland T (2011) Geological framework of the mineral deposits of the collahuasi district, región de tarapacá, chile. PhD thesis, University of Tasmania
- Van den Kerkhof AM, Hein UF (2001) Fluid inclusion petrography. *Lithos* 55(1-4):27–47
- Klyukin YI, Steele-MacInnis M, Lecumberri-Sanchez P, Bodnar RJ (2019) Fluid inclusion phase ratios, compositions and densities from ambient temperature to homogenization, based on pvtx properties of h₂onacl. *Earth-Science Reviews* p 102924
- Lee A (1994) Evolution of the rosario copper-molybdenum porphyry deposit and associated copper-silver vein system. Collahuasi district, I region, northern Chile: Unpublished MA thesis, Kingston, Ontario, Canada, Queens University
- Masterman G (2003) Structural and geochemical evolution of the rosario cu-mo porphyry deposit and related cu-ag veins, collahuasi district, northern chile: Unpublished ph. d. Unpublished Ph D thesis p 253
- Masterman GJ, Cooke DR, Berry RF, Clark AH, Archibald DA, Mathur R, Walshe JL, Durán M (2004) 40ar/39ar and re-os geochronology of porphyry copper-molybdenum deposits and related copper-silver veins in the collahuasi district, northern chile. *Economic Geology* 99(4):673–690
- Masterman GJ, Cooke DR, Berry RF, Walshe JL, Lee AW, Clark AH (2005) Fluid chemistry, structural setting, and emplacement history of the rosario cu-mo porphyry and cu-ag-au epithermal veins, collahuasi district, northern chile. *Economic Geology* 100(5):835–862
- Moore RL, Masterman G (2002) The corporate discovery history and geology of the collahuasi district porphyry copper deposits, chile. In: *Giant Ore Deposits: characteristics, genesis and exploration*, vol 1, pp 23–50
- Munchmeyer C, Hunt J, Ware H (1984) Geología del distrito de collahuasi y del pórfido cuprífero rosario
- Nash JT (1976) Fluid-inclusion petrology—data from porphyry copper deposits and applications to exploration: a summary of new and published descriptions of fluid inclusions from 36 porphyry copper deposits and discussion of possible applications to exploration for copper deposits. US Govt. Print. Off.
- Roedder E (1972) Composition of fluid inclusions. Tech. rep.
- Roedder E (1984) Volume 12: Fluid inclusions. *Reviews in mineralogy* 12
- Roedder E (1990) Fluid inclusion analysis—prologue and epilogue. *Geochimica et Cosmochimica Acta* 54(3):495–507
- Roedder E (1997) Fluid inclusion studies of hydrothermal ore deposits. *Geochemistry of hydrothermal ore deposits*
- Sillitoe RH (2010) Porphyry copper systems. *Economic geology* 105(1):3–41
- Singer DA, Berger VI, Moring BC, Groat CG (2002) Porphyry copper deposits of the world: Database, maps, and preliminary analysis. Citeseer
- Vergara H (1978) Cuadrángulo ujina, región de tarapacá, carta geológica de chile, escala 1: 50,000
- Vergara H, Thomas A (1984) Hoja collacagua, 1: 250000. *Carta Geol Chile* 59
- Wahler W (1956) Über die in kristallen eingeschlossenen flüssigkeiten und gase. *Geochimica et Cosmochimica Acta* 9(3):105–135
- Williams TJ, Candela PA, Piccoli PM (1995) The partitioning of copper between silicate melts and two-phase aqueous fluids: an experimental investigation at 1 kbar, 800 c and 0.5 kbar, 850 c. *Contributions to Mineralogy and Petrology* 121(4):388–399
- Yardley BW, Bodnar RJ (2014) Fluids in the continental crust. *Geochemical Perspectives* 3(1):1–2
- Zajacz Z, Halter W (2009) Copper transport by high temperature, sulfur-rich magmatic vapor: Evidence from silicate melt and vapor inclusions in a basaltic andesite from the villarrica volcano (chile). *Earth and Planetary Science Letters* 282(1-4):115–121
- Zajacz Z, Seo JH, Candela PA, Piccoli PM, Tossell JA (2011) The solubility of copper in high-temperature magmatic vapors: a quest for the significance of various chloride and sulfide complexes. *Geochimica et Cosmochimica Acta* 75(10):2811–2827
- Zajacz Z, Candela PA, Piccoli PM (2017) The partitioning of cu, au and mo between liquid and vapor at magmatic temperatures and its implications for the genesis of magmatic-hydrothermal ore deposits. *Geochimica et Cosmochimica Acta* 207:81–101

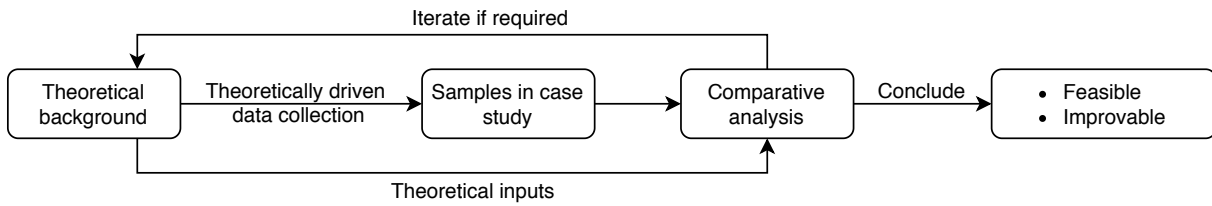


Figure 1: Scheme of exploring the potential of fluid inclusions in porphyry copper deposits. Feedback between comparative analysis and theoretical background made to improve the robustness of the derived conclusions.

Table 1: Intrusives of study area and their relationship with mineralization

Intrusive	Age	Composition	Relationship
Porphyry Rosary (PRO)	34.2 - 32.9 Ma	Quartz - monzonite	Syn - mineralization
Porphyry Collahuasi (PCO)	59 Ma	Quartz - monzonite	Pre - mineralization
Porphyry Ines (PIN)	Permian - Triassic	Dacite	Pre - mineralization

Table 2: Number of samples in which the presence of the fluid inclusion type was observed. A sample can present more than one type. L: liquid, V: vapour, H: halite, Ccp: Cachopirite, X: opaque metals

Type Fluid inclusion	Type 0 L-rich	Type 1 L+H	Type 2 L+Ccp	Type 3 L+X	Type 4 L+V+H	Type 5 L+V	Type 6 V-rich
Frequency	171	70	24	40	30	176	188

Table 3: List of samples used in [Figure 14](#), [Figure 15](#) and [Figure 16](#). PRO: Porphyry Rosario, *: moot.

Sample	Code	Depth m.a.s.l	Type of main Fluid inclusion	Type of Vein	Rock	Represent
#1	NA - 4	4.345	Type 6	B	PRO	serie 1
#2	NA - 88	4.165	Type 6	B*	PRO	serie 1
#3	NA - 7	4.130	Type 4	B	PRO	serie 1
#4	VD180310	4.090	Type 5	B	PRO	serie 1
#5	NA - 15	4.010	Type 0	D	PRO	serie 1
#6	VD670510	3.773	Type 6	B	PRO	serie 2
#7	DM - 11	3.743	Type 5	B	PRO	serie 2
#8	VD690510	3.650	Type 5	B	PRO	serie 2
#9	DM - 14	3.577	Type 4	B	PRO	serie 2
#10	VD540510	3.490	Type 6	B	PRO	serie 2

<p>(a) Fluid inclusion</p>  <p>Description</p> <p>Fluid of moderate density with precipitation of chalcopyrite from the trapped fluid.</p> <p>Location in porphyry system</p> <p>Characteristics of early stages in central and deep places.</p>	<p>(b) Fluid inclusion</p>  <p>Description</p> <p>Low density fluid with chalcopyrite precipitation, also named low salinity vapor.</p> <p>Location in porphyry system</p> <p>Characteristics of the shallowest part in early stages.</p>
<p>(c) Fluid inclusion</p>  <p>Description</p> <p>High density fluid of low to moderate salinity (diluted liquid).</p> <p>Location in porphyry system</p> <p>Early stages in the deepest and most central part, or late stages in the most shallow and central part.</p>	<p>(d) Fluid inclusion</p>  <p>Description</p> <p>High salinity fluid and copper concentration favoring the chalcopyrite and halite (brine) precipitation.</p> <p>Location in porphyry system</p> <p>Vertically distributed in intermediate stages from the surface to the depth and laterally from the center to the periphery, useful as a limiter of mineralization area.</p>
<p>(e) Fluid inclusion</p>  <p>Description</p> <p>Coexistence of low-density fluids with fluids of high salinity and copper concentration, characterizes boiling event (characteristic of copper porphyry deposits).</p> <p>Location in porphyry system</p> <p>Characteristic of the central part of the porphyry.</p>	<p>(f) Fluid inclusion</p>  <p>Description</p> <p>Coexistence of high and low density fluids, characteristic of boiling events.</p> <p>Location in porphyry system</p> <p>Initial stages of a porphyric system characterized by boiling. Presented in the superficial zone, with the presence of chalcopyrite, it is the deepest zone.</p>

Figure 2: Schematic petrographic observation at room temperature of 6 different fluid inclusions with their description and association with respect to the copper porphyry type system. A, B, C, D: individual fluid inclusions. F and G: coexistence of fluid inclusions, and evidence boiling. Black fill: water steam; Triangle: chalcopyrite; Square: Halite; White space inside: liquid.

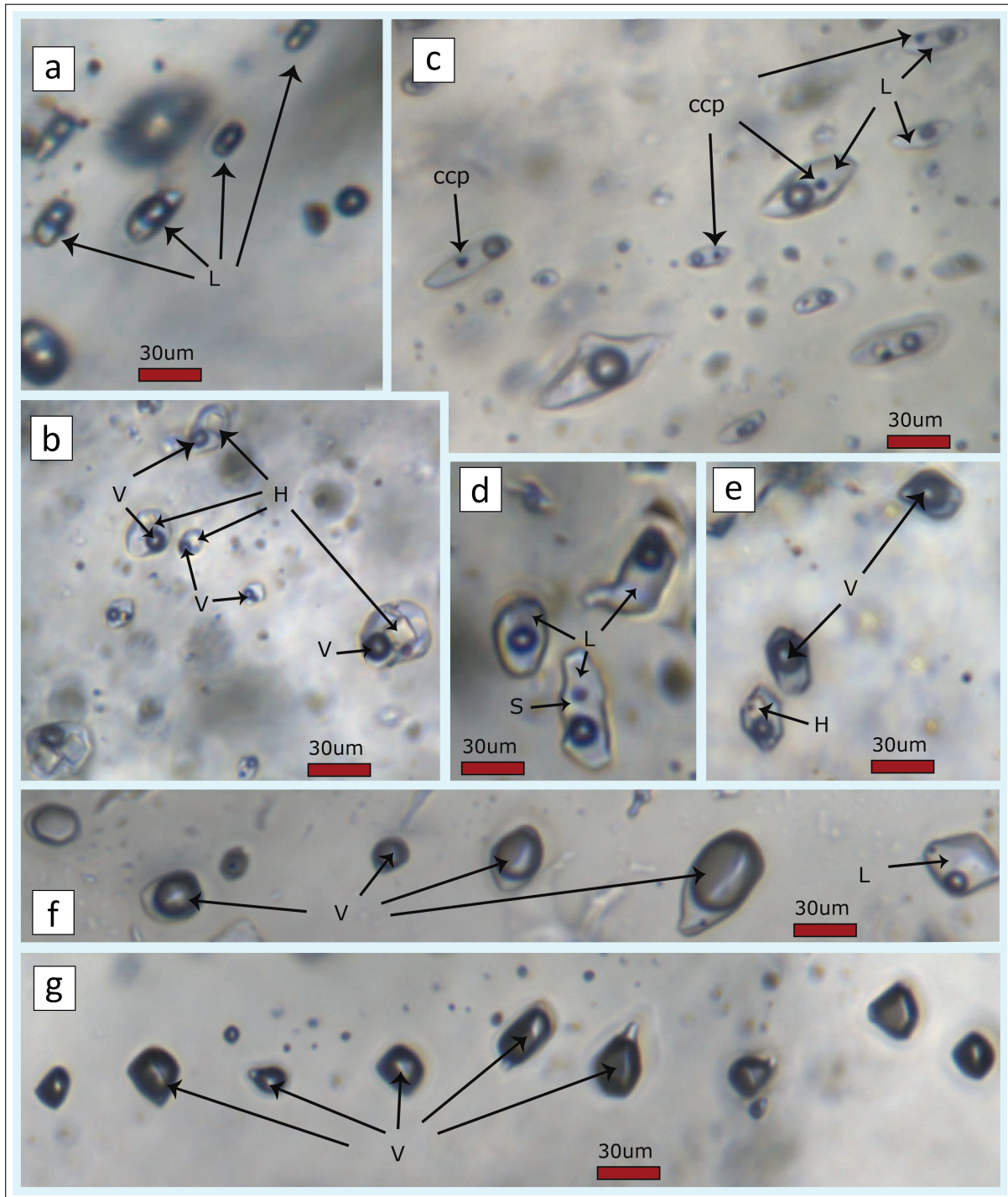


Figure 3: Types of fluid inclusions seen and defined in this work. They are classified and described as: (a) type 0, family of liquid-rich inclusions. (b) type 1, family of liquid-rich inclusions with halite precipitation. (c) type 2, family of liquid-rich inclusions, with sales and metal saturation, precipitating halite and chalcopyrite. (d) type 3, liquid-rich inclusions with precipitation of opaque solids, difficulty in distinguishing as chalcopyrite, indicating saturation of metals or metals in the fluid. (e) type 4, coexistence of inclusions rich in steam and inclusions with the presence of halite. (f) type 5, coexistence of vapour-rich inclusions with liquid-rich inclusions, characteristic of boiling. (g) Type 6, family of fluid rich in vapour or low-density inclusions, characteristic of rapid boiling, flashing. V: vapour, L: liquid, ccp: chalcopyrite, S: solid, H: halite.

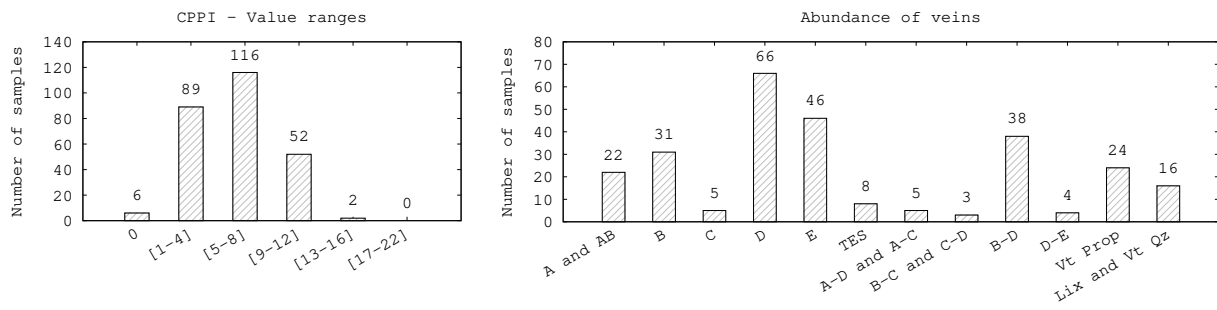


Figure 4: Histogram of data. CPPI value ranges (left) and abundance of veins (right).

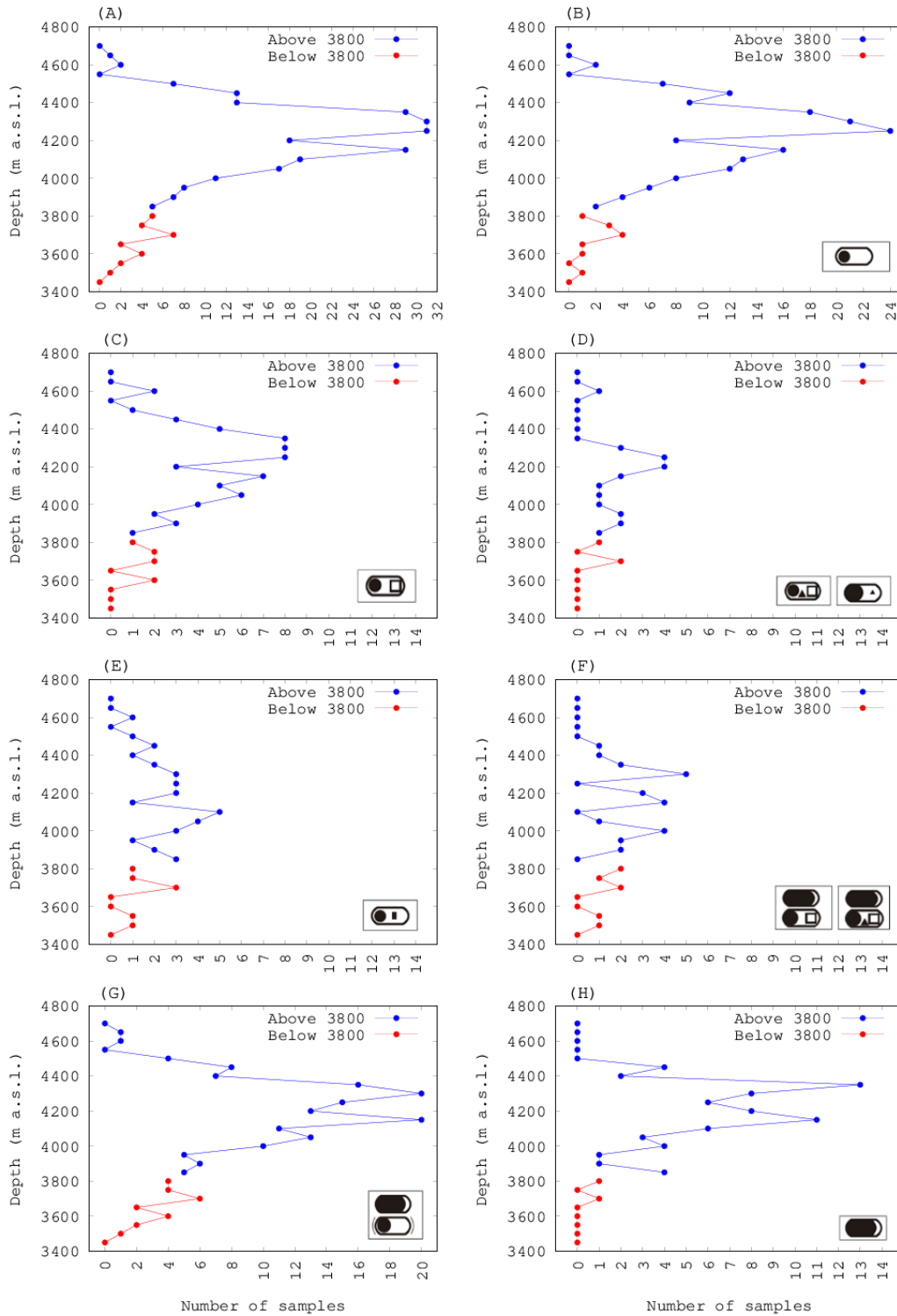


Figure 5: General graph of the distribution of the samples based on the depth expressed in meters above sea level, Y axis, (m a.s.l.). The X axis corresponds to the number of samples associated at that level. In blue it is considered shallow area and in red deep area. The division is around 3800m a.s.l. Each case evaluates all the samples independently, so the same sample can be counted in several graphs. Graph (a) corresponds to the general distribution of the samples studied in the investigation. The fluid inclusion evaluated is visually expressed in the lower right with its representation at room temperature, corresponding as follows: (b) Type 0 ; (c) Type 1 ; (d) Type 2 ; (e) Type 3 ; (f) Type 4 ; (g) Type 5 ; (h) Type 6.

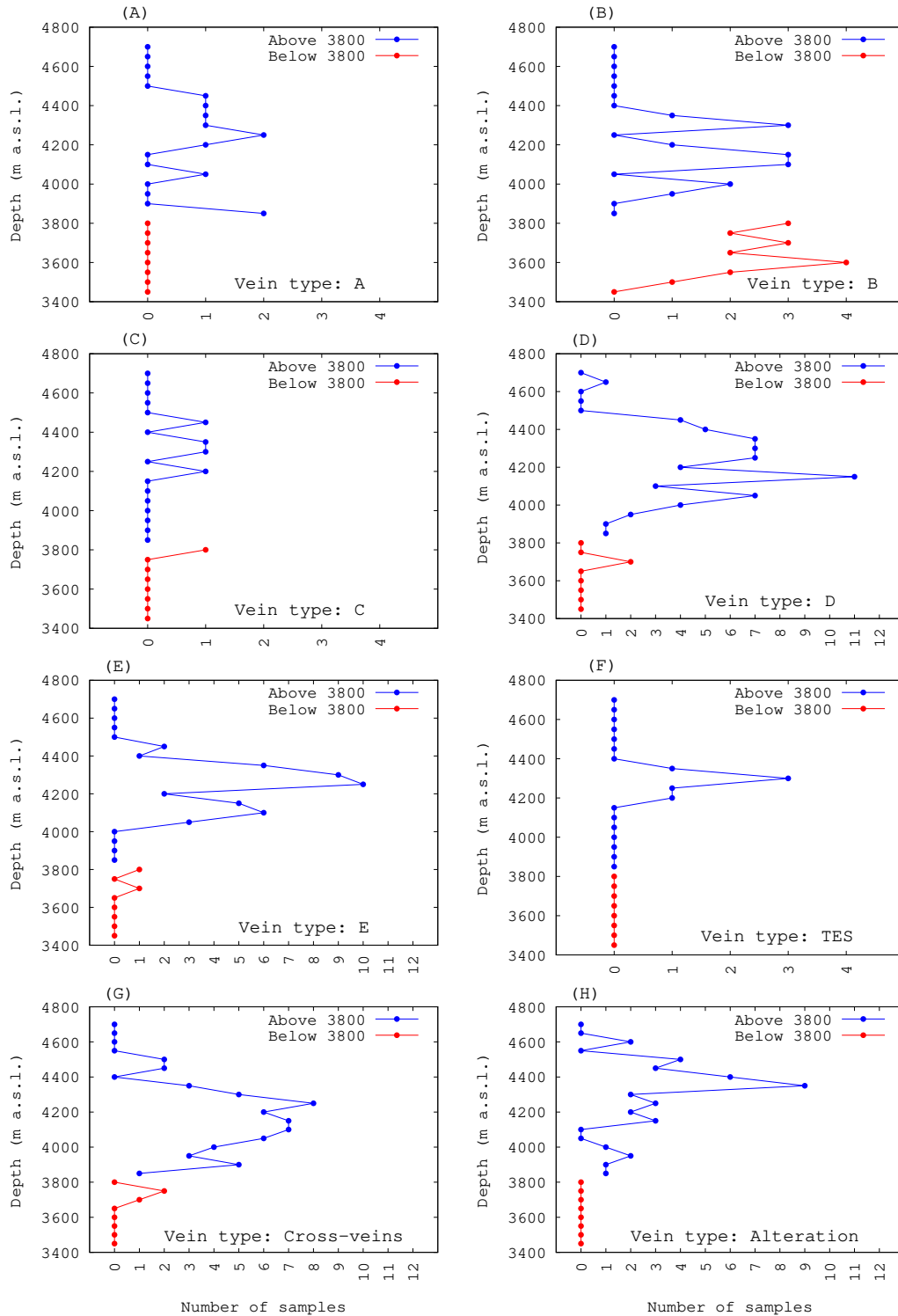


Figure 6: General graph of the distribution of the samples based on the depth expressed in meters above sea level, Y axis, (m a.s.l.). The X axis corresponds to the number of samples associated at that level. In blue it is considered shallow area and in red deep area. The division is around 3800m a.s.l. Each case evaluates all the samples independently, so the same sample can be counted in several graphs. The vein type is expressed in the lower right with, corresponding as follows: (a) Type A (b) Type B (c) Type C (d) Type D (e) Type E (f) Type TES (g) Type cross-vein (h) Type Alteration. The predominance of type B veins in the deep zone is notable.

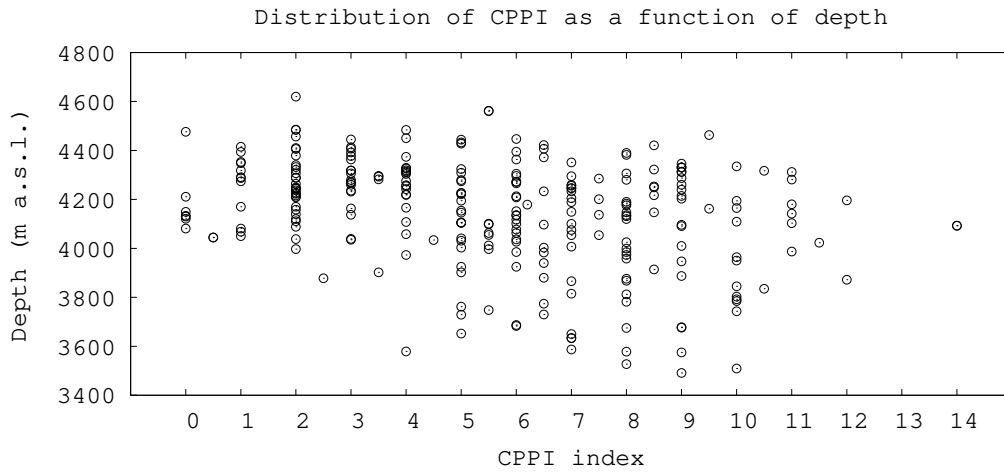


Figure 7: Distribution of CPPI as a function of depth (meters above sea level)

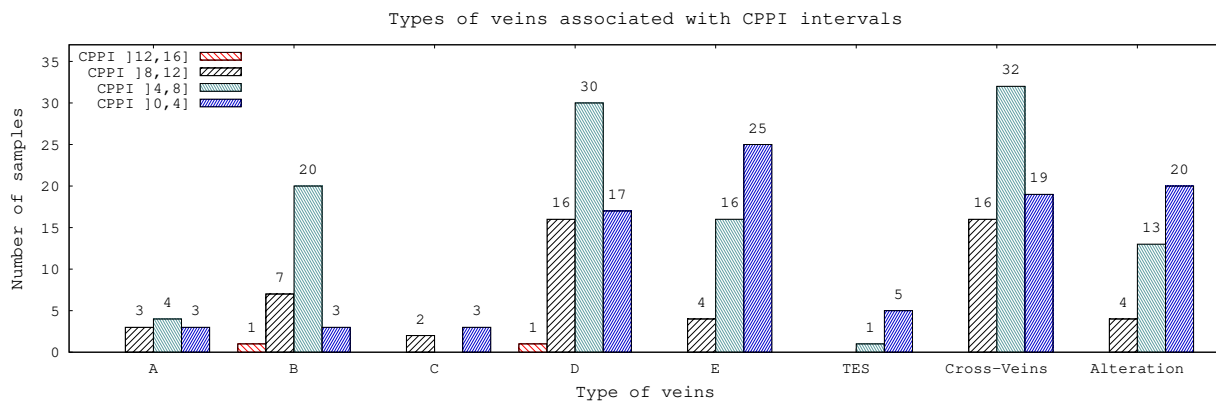


Figure 8: Number of samples associated with the manifestation of two assigned variables: The vein type present and its CPPI value. According to its CPPI it is grouped into intervals, displayed as bars. Where a bar is missing it means that there were no samples with such a vein type that it presents a CPPI value of the missing range.. The Y axis expresses the total number of samples that meet this relationship. Example: 20 samples that present type B vein have a CPPI value in the range]4-8]

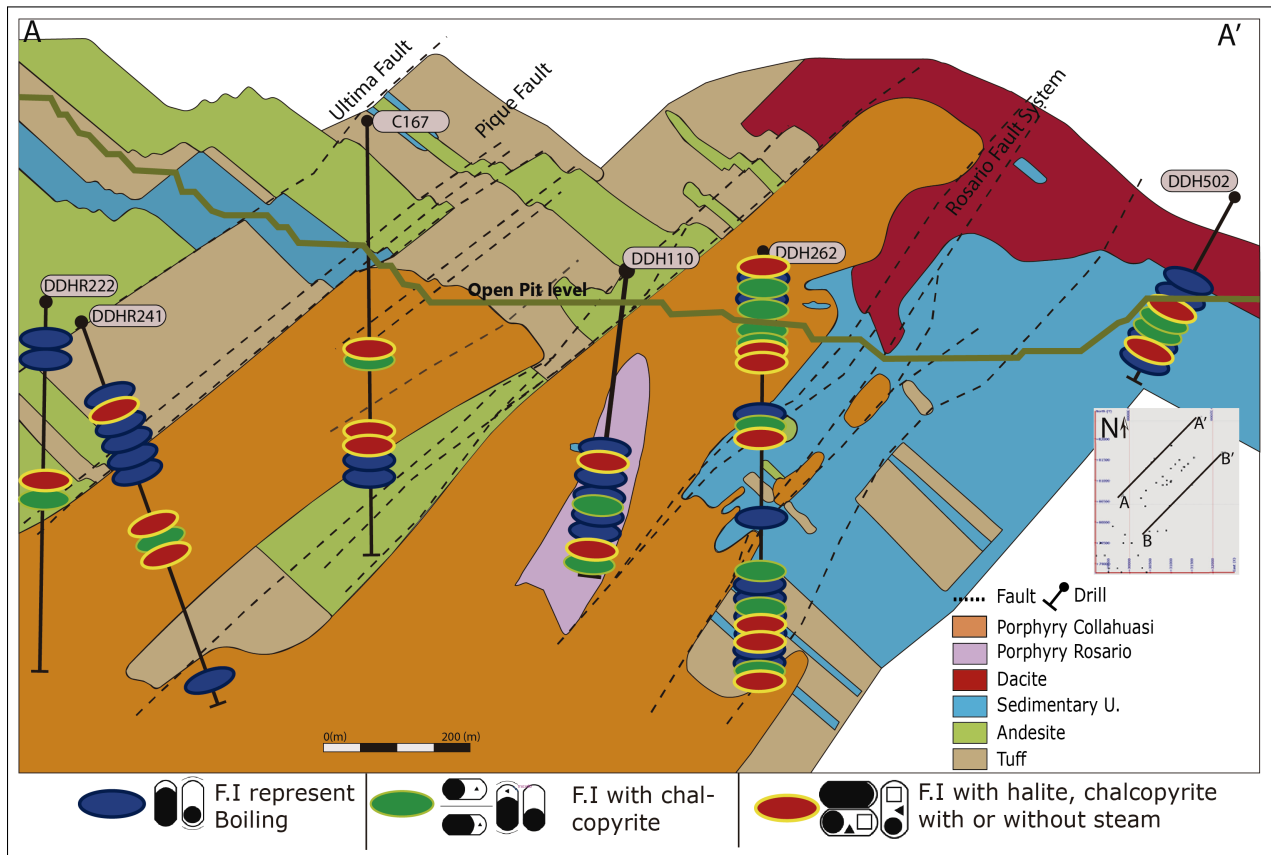


Figure 10: Graphic distribution in AA' profile of the inclusions that show boiling (type 5, blue), inclusions that present chalcopyrite (type 2 and 3, green) and inclusions with halite and chalcopyrite, coexisting or not with steam-rich inclusions (type 1 and type 4, red). Intense boiling near faults and rosary porphyry lithology.

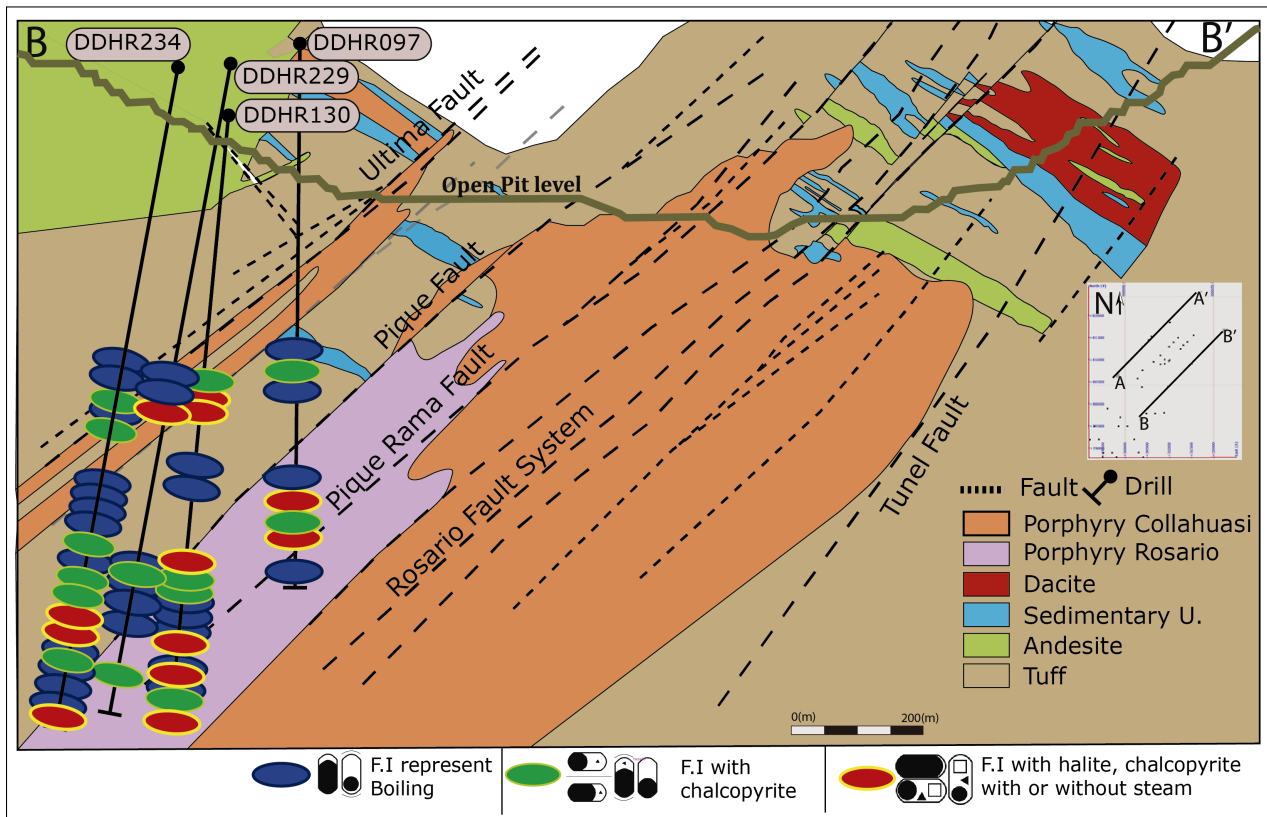


Figure 11: Graphic distribution in BB' profile of the inclusions that show boiling (type 5, blue), inclusions that present chalcopyrite (type 2 and 3, green) and inclusions with halite and chalcopyrite, coexisting or not with steam-rich inclusions (type 1 and type 4, red). A portion of inclusions with saturation of halite and chalcopyrite, with evidence of boiling, are location on middle in the rosary porphyry lithology. Other portion are close to faults.

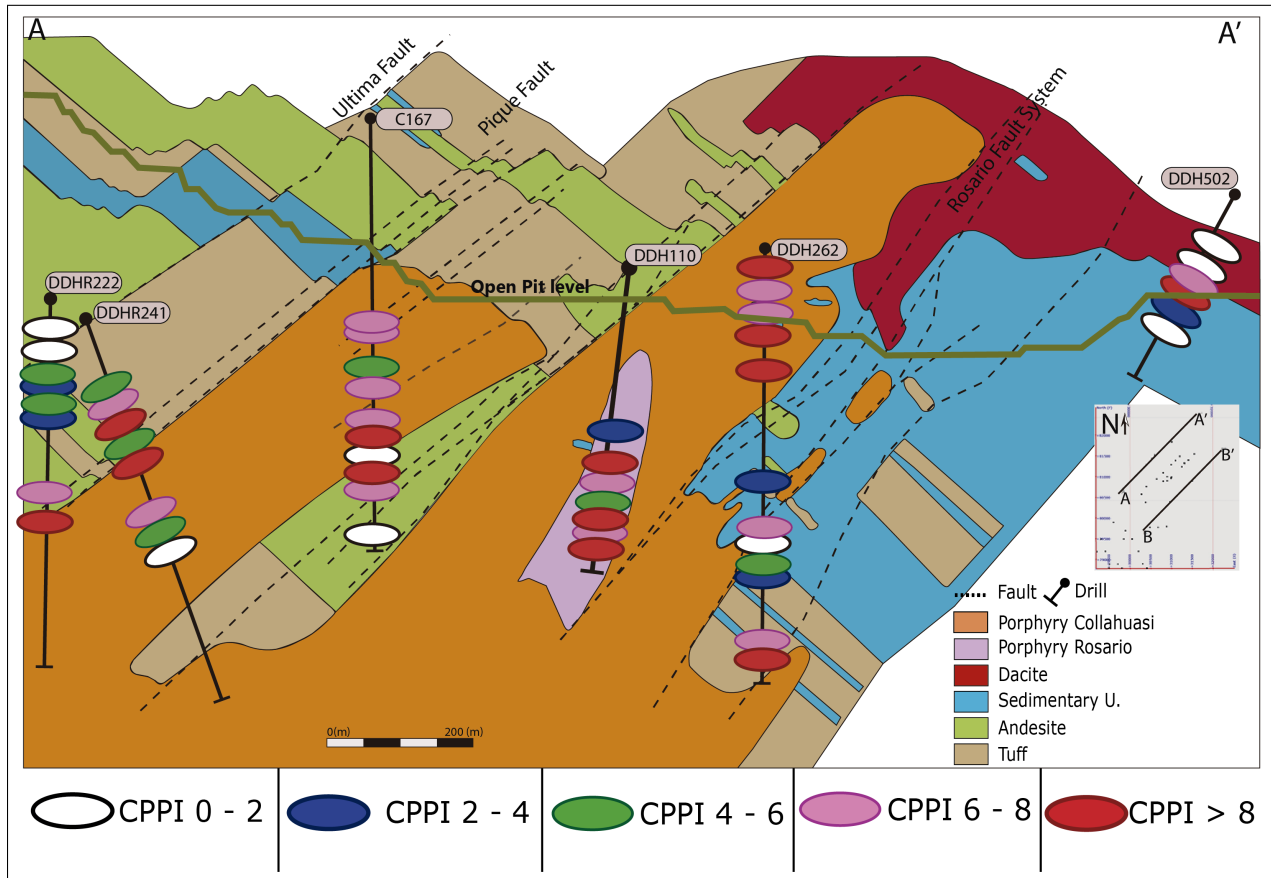


Figure 12: Graphical distribution in AA 'profiles of the copper porphyry probability index values (CPPI) in the Rosario porphyry area. Low values, represented by white ovals, stand out in the sectors furthest from the porphyry Rosario lithology, however in these distant sectors high values, represented by red ovals, stand out that could be related to the presence of the structures, faults, in their proximity.

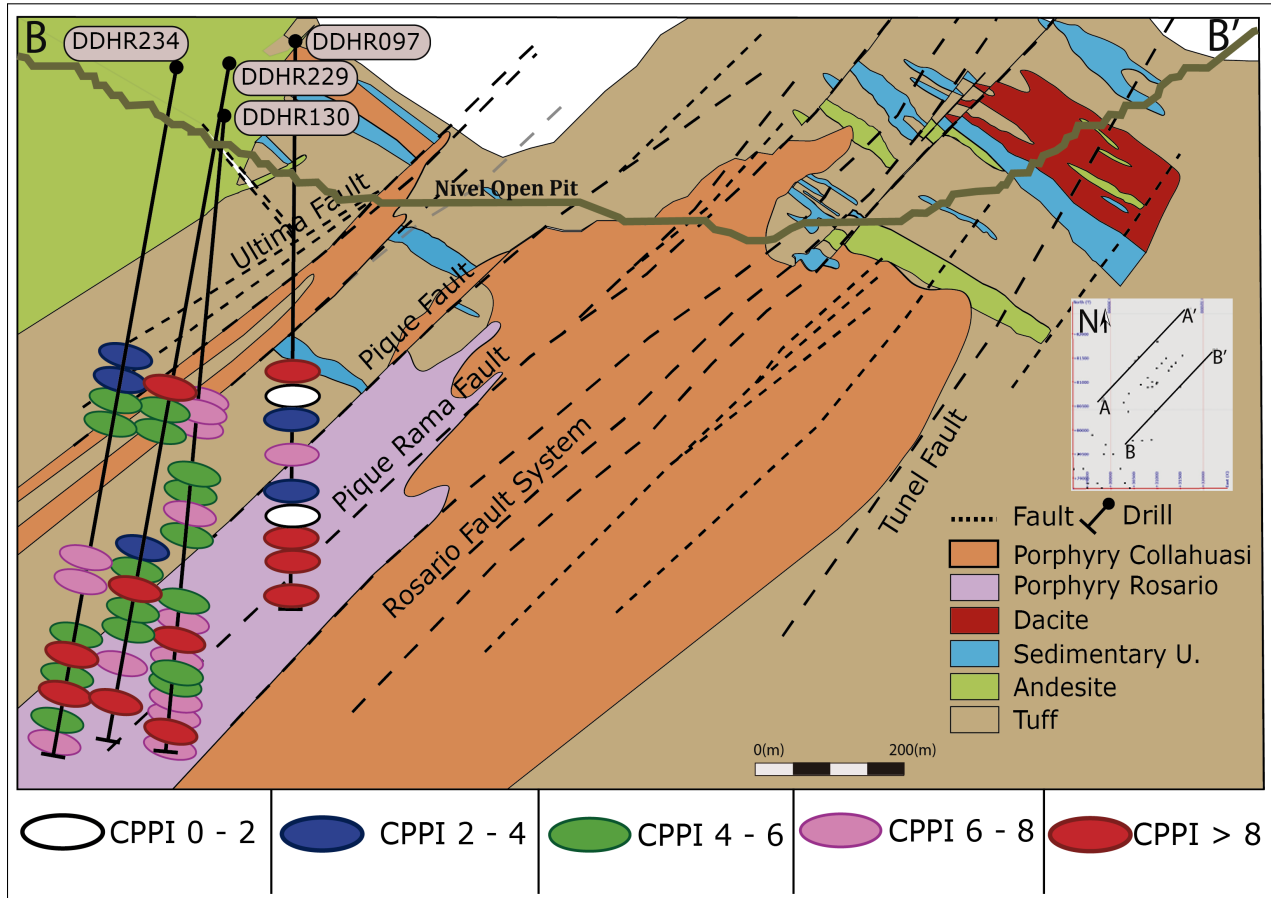


Figure 13: Graphical distribution in the BB' profiles of the copper porphyry probability index values (CPPI) in the Rosario porphyry area. A positive correlation of the high values, represented by red ovals, is observed in samples corresponding to the rosary porphyry lithology. An alignment can be interpreted with respect to the fault "pique rama" in the center of the lithological zone of interest, and with SW direction that could be continued in depth.

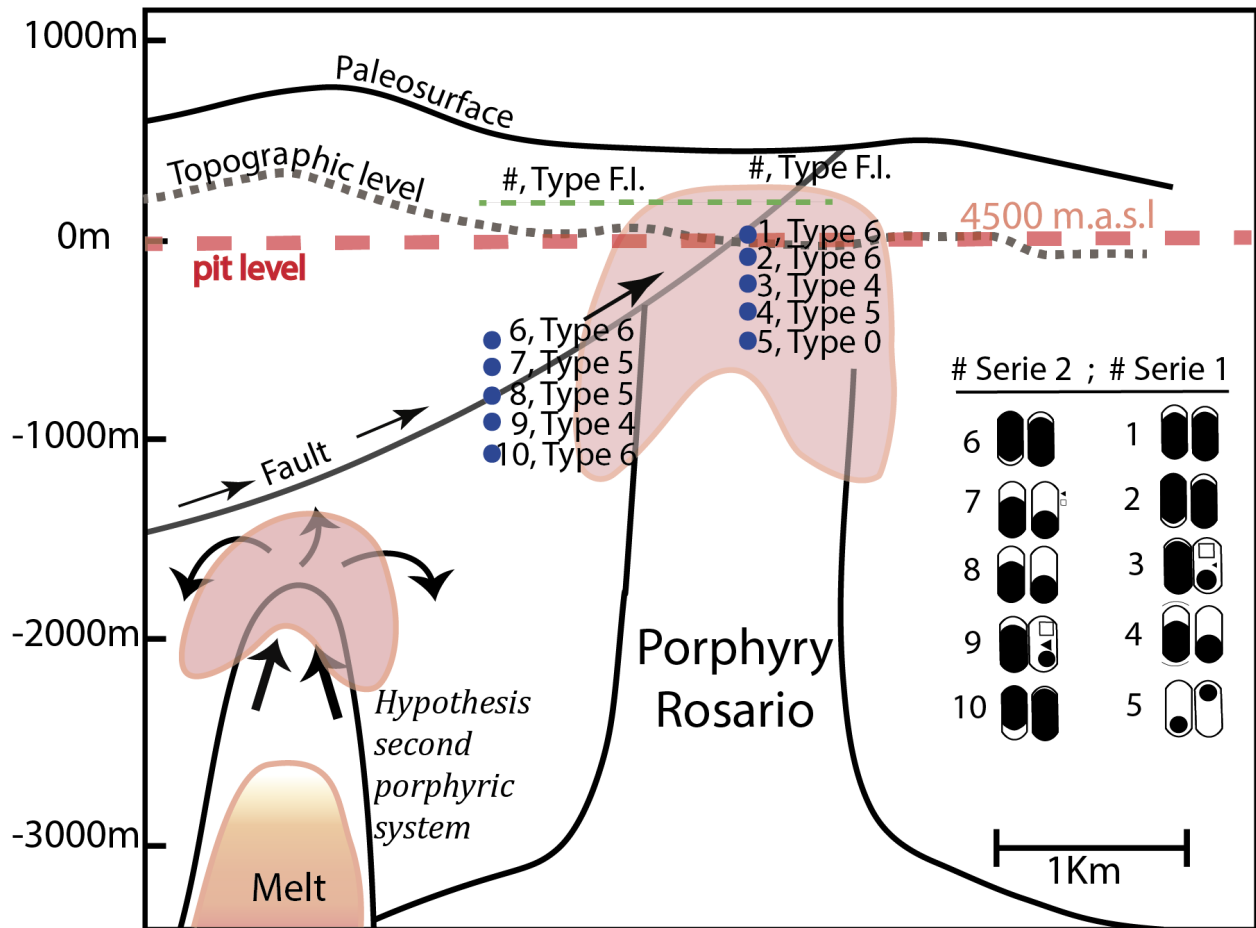


Figure 14: Graphical distribution of the sample collection in Table 3. Each sample is worked with the most predominant type of fluid inclusion. They are worked as series 1 and 2, which describe a vertical distribution, or failing that, as a sequence. Series 1, corresponds to the shallow-central part of the rosary porphyry system, series 2 represents the deepest part and is located in the most southwestern sectors with respect to series 1. Segmented red line indicates the current horizon of the mine, the which is at a height of 4,500 m.a.s.l. Illustration taken, modified and used to solve the hypotheses established by Masterman et al. (2005) from the observations and methodologies of this work.

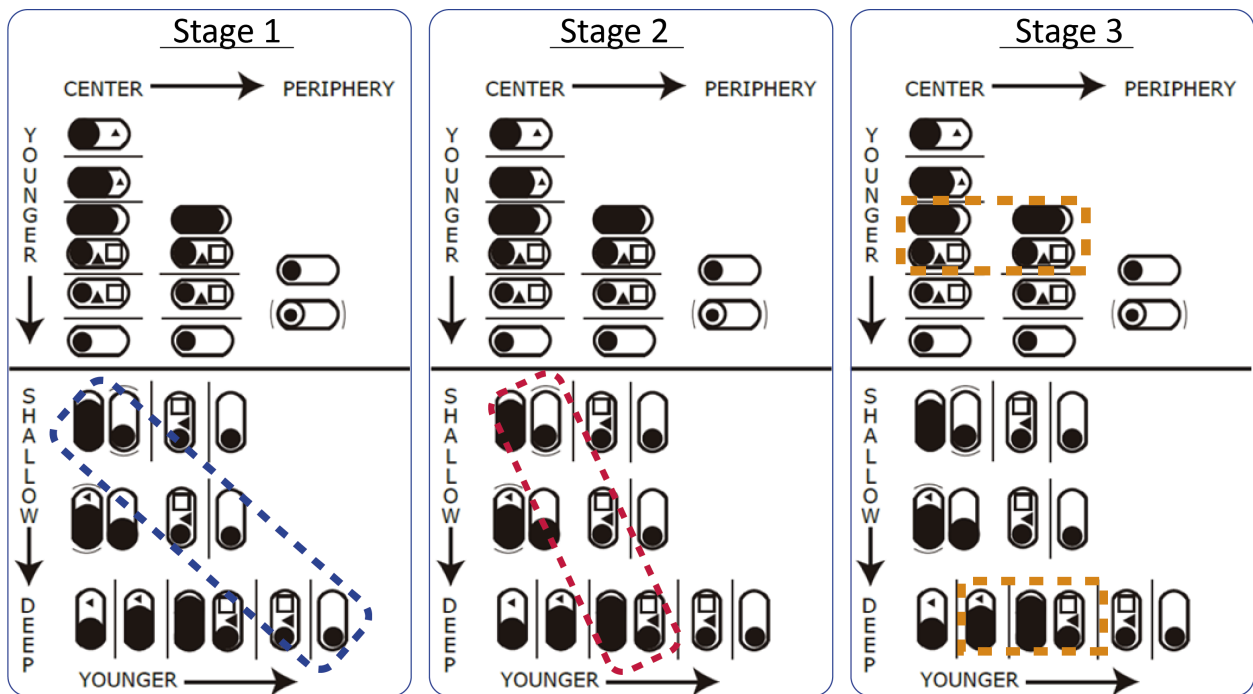


Figure 15: Analysis of porphyry location using fluid inclusions petrography. Each scenario is supported with the observations and analyzes of the 10 samples presented in Table 3, where they can be considered as a single continuous series from the shallowest to the deepest zone (union of series 1 to series 2, stage 3) or each series represent separate scenarios of vertical distribution (stage 1 and 2 to series 1 and 2 respectively). Stage 1 and 2 represent a discussion without considering time as a fixed variable for the development and formation of the Rosario deposit, stage 3 considers the fixed time to develop the porphyry system studied.

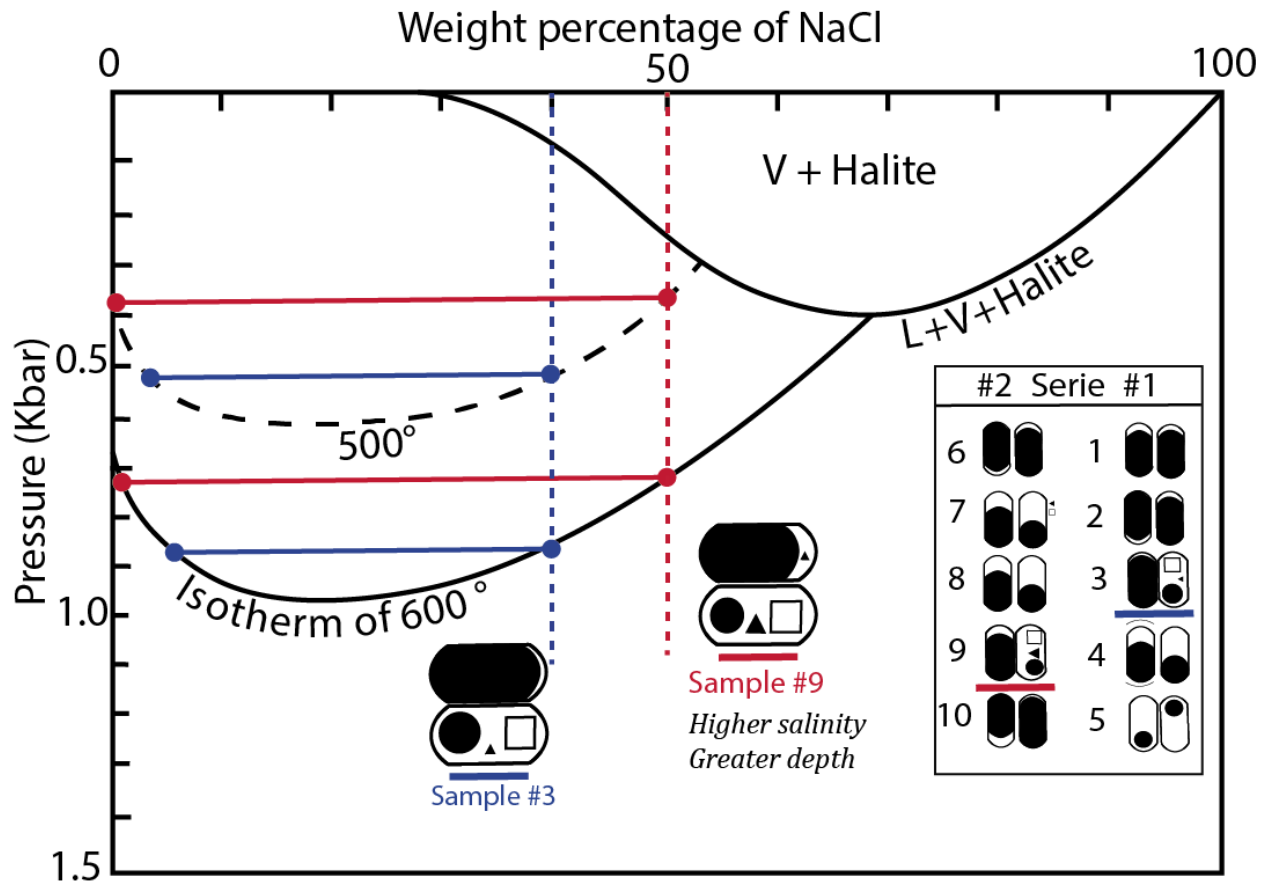


Figure 16: Pressure-weight% NaCl graph in H₂O-NaCl system, with referential isotherms of 600C and 500C. Depending on the salinity, an isotherm is traversed and it has an associated pressure. The percentage of NaCl can be estimated comparatively by the size of the halite observed in an inclusion at room temperature. Sample # 9 higher salinity and deeper than # 3. L: liquid, V: vapour. Lines red and blue, represent location of each samples on isotherm, in case of correspond.